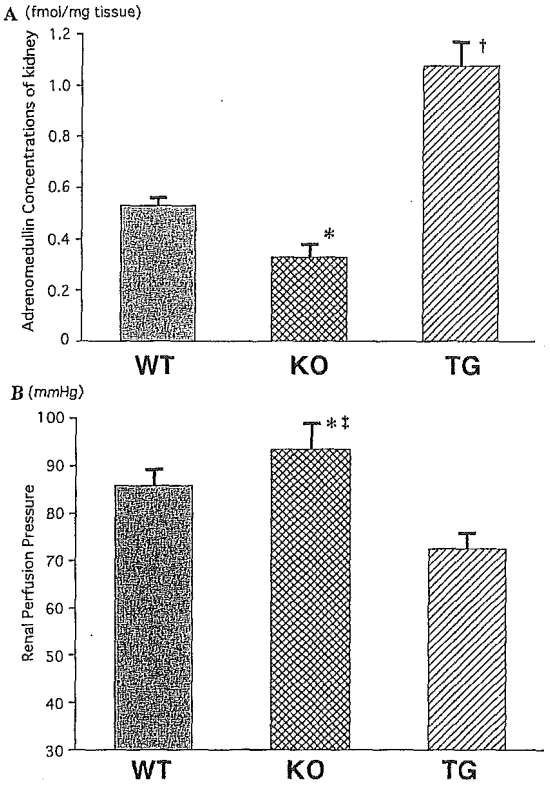

Figure 1. Adrenomedullin (AM) concentrations of the kidneys (A) and baseline renal perfusion pressure (B) isolated from AM transgenic (TG) mice, AM knockout (KO) mice, and wild-type (WT) mice. *$P<0.01$, †$P<0.001$ vs WT; ‡$P<0.001$ vs TG.

Kruskal-Wallis test was used. Differences with a value of $P<0.05$ were considered statistically significant.

Results

Renal Contents of AM

We measured the renal contents of AM in the 3 groups of mice by RIA. As shown in Figure 1A, AM contents in the kidney of AM TG mice were significantly greater than WT mice, whereas those of AM KO mice were significantly less. These results were compatible with the findings of our previous reports.[14,15]

Isolated Perfused Kidney

Kidneys from KO, TG, and WT mice were macroscopically normal and their weight did not greatly differ among the 3 groups. Baseline RPP in KO mice was significantly higher, whereas that in TG mice was lower, compared with RPP in WT mice kidneys (Figure 1B).

Figure 2 shows the effects of ACh on RPP and NO release in the 3 groups of mice kidneys. ACh lowered RPP of kidneys in either group in a dose-related manner. The degree of renal vasodilation caused by ACh was smaller in TG mice than in WT and KO mice. The ACh-induced vasodilation was associated with an increase in NO release from the kidney. NO release caused by ACh was greater in TG mice and smaller in KO mice, compared with WT mice. Thus, TG mice kidneys showed hyporesponsiveness to NO. The responses to AM in the 3 groups of mice were similar to those to ACh (data not shown). Figures 3A and 3B shows the effects of AM receptor antagonists AM(22-52) and CGRP(8-37) on RPP, respectively. Both antagonists alone significantly elevated RPP in a dose-related fashion. The increase in RPP was significant even in KO and WT mice. The response decreased in the following order: TG>WT>KO.

In order to explore the involvement of the NO-cGMP pathway in AM-induced vasodilation, we examined the effects of L-NMMA and E-4021 on RPP. As shown in Figure 3C, L-NMMA alone increased RPP in all 3 groups of kidneys. In contrast, E-4021 alone reduced RPP (Figure 3D). These changes in RPP caused by L-NMMA and E-4021 were dose-related and the responses decreased in the following order: TG>WT>KO.

Ischemic Acute Renal Failure

No mice died after renal ischemia/reperfusion. Serum concentrations of urea nitrogen markedly increased 24 hours after reperfusion in WT mice (Figure 4A). Decreases in renal excretory function were significantly greater in KO mice than in WT mice. However, the increases in urea nitrogen levels were significantly smaller in TG mice. Serum creatinine levels changed almost in parallel with urea nitrogen levels in the 3 groups of mice (Figure 4B). Pretreatment with L-NAME did not change the increases in serum urea nitrogen levels in WT and KO mice, whereas it significantly increased them in TG mice, resulting in no differences in serum urea nitrogen or creatinine levels among the 3 groups of mice.

Changes in renal excretory function induced by ischemia were confirmed by histological analysis. Figure 5 shows the renal histology of the 3 groups of mice. In WT mice, marked damage of renal tissues, particularly in the tubuli, were observed; these included detachment of epithelial cells of the proximal tubuli, interstitial edema, and tubular casts. Expansion of Bowman's space was also observed. AM KO mice also had marked tubular damage. However, in AM TG mice

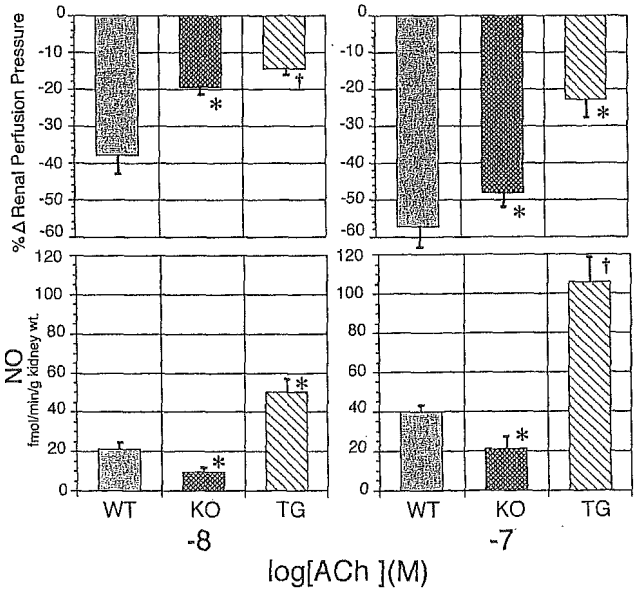

Figure 2. Effects of acetylcholine (ACh) on renal perfusion pressure (RPP) and release of NO in TG, WT, and KO mice. *$P<0.05$, †$P<0.01$ vs WT.

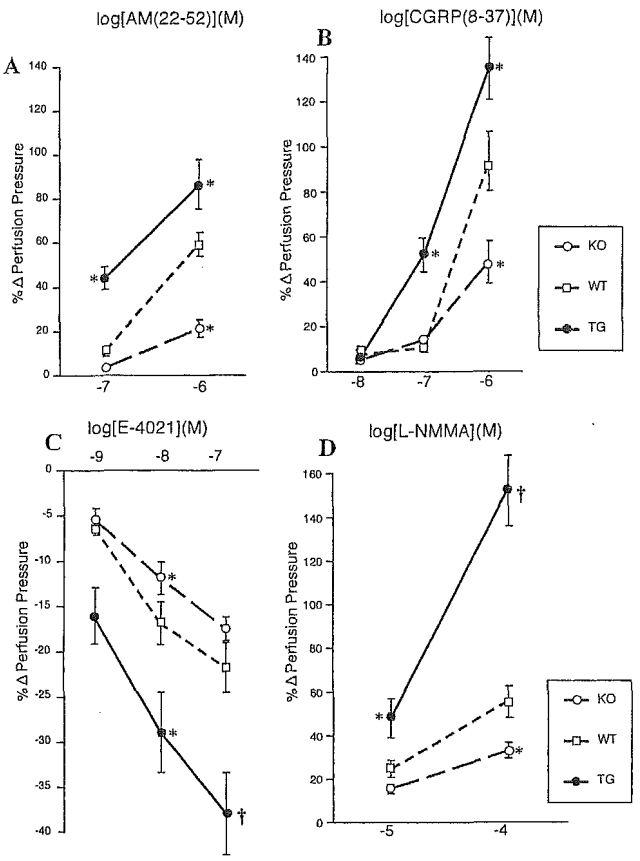

Figure 3. Effects of adrenomedullin (AM) receptor antagonists, AM(22-52) (A) and CGRP(8-37) (B), on renal perfusion pressure (RPP) in TG, WT, and KO mice. Effects of E-4021 (C) and N^G-monomethyl-L-arginine (L-NMMA) (D) on renal perfusion pressure (RPP) in TG, WT, and KO mice. *$P<0.05$, †$P<0.01$ vs WT.

renal injury was apparently mild. In fact, all 4 types of damage scores were significantly less marked in TG mice compared with the other 2 groups of mice. Figure 6 shows the means of 4 types of injury scores in each group of mice. AM KO mice kidneys subjected to ischemia showed significantly greater scores than WT mice and AM TG mice. Pretreatments with L-NAME also diminished differences in renal injury scores among the 3 groups of mice.

Renal NOS Activity

As shown in Figure 7, calcium-dependent NOS activity in the renal medulla was greater in TG mice, whereas it tended to be less in KO mice. Ischemia/reperfusion decreased the NOS activity in all 3 groups of mice. However, the NOS activity was still greater in TG mice kidneys. On the other hand, calcium-independent NOS activity was not detected in the kidney of any group of animals.

Discussion

Endothelial cells secrete many circulating and local vasoactive hormones. Among them, endothelin-1 and NO are potent vasoconstrictive and vasodilative substances, respectively, and they play important roles because their gene disruption results in death or in a hypertensive reaction, respectively.[25,26] However, it has not been clarified whether endothelium-derived AM is a significant factor in the regulation of circulation.

The plasma concentration of AM in healthy subjects is at a picomolar level.[1,7] However, the vasodilatory effects of AM appear at concentrations higher than 10^{-10} mol/L, according to previous reports.[14] In the present study, significant vasodilation in the renal vessels and aorta was observed also at about 10^{-9} mol/L. That is, the physiological circulating level of AM is about a hundredth of the effective concentration on arteries, although it is possible that the vascular wall may be exposed to locally high concentrations of AM. Receptor antagonists are useful tools to explore the role of endogenous ligands. We examined 2 kinds of AM receptor antagonists, CGRP(8-37)[27] and AM(22-52).[5] Both antagonists increased the vascular tone in renal vessels precontracted by angiotensin II in a dose-related manner. This suggests that endogenous AM in the vasculature shows tonic inhibition on vasoconstrictive stimuli. This phenomenon may be explained by some agonistic action of the antagonists, particularly at higher concentrations. In fact, AM(1-25), a truncated peptide of AM, exerts vasoconstrictive activity.[28] However, CGRP derivatives have not been reported to cause vasoconstriction.

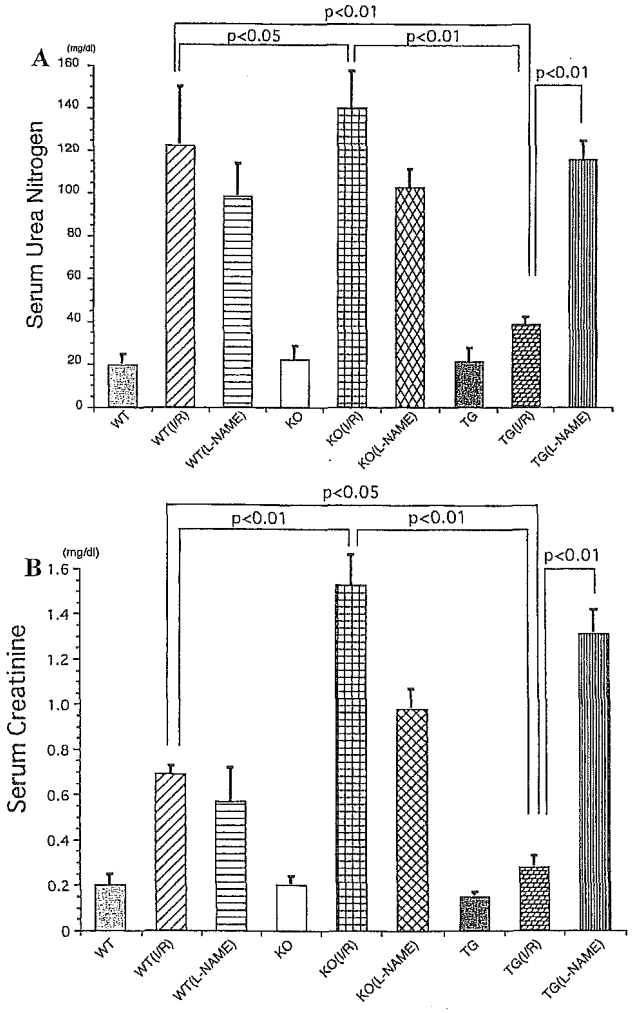

Figure 4. Serum urea nitrogen (A) and creatinine levels (B) in mice with ischemic acute renal failure. (I/R) indicates ischemia/reperfusion; L-NAME, N^G-nitro-L-arginine methyl ester+I/R.

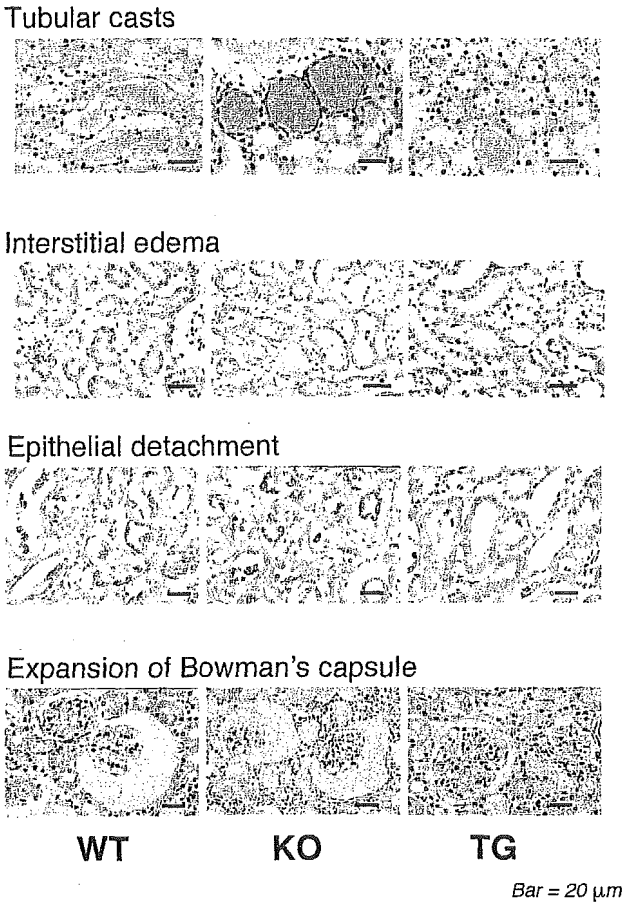

Figure 5. Photographs of renal histology showing tubular casts, interstitial edema, epithelial detachment, and expansion of Bowman's capsule from AM transgenic (TG) mice, AM knockout (KO) mice, and wild-type (WT) mice.

Furthermore, because endothelial denudation of the aorta diminished the vasoconstriction caused by receptor antagonists (unpublished observation, 2001), it is unlikely that the two antagonists per se increased vascular tone. Thus, it appears that the antagonists-induced vasoconstriction is attributed to a direct blockade of the action of endogenous AM.

It is striking that the receptor antagonists significantly increased RPP even in WT mice, although vasoconstriction was greater in TG mice and less in KO mice. Baseline perfusion pressure in the kidney isolated from KO mice was significantly higher than that from WT mice. These findings suggest that endogenous AM actually regulates renal vascular tone under physiological conditions, at least in mice. Furthermore, the decrease in endogenous AM production by 50% may contribute to increases in renal vascular resistance. It is not exceptional that a 50% reduction of gene expression influences its function. For example, heterozygote eNOS KO mice showed slightly higher blood pressure[29] and greater susceptibility to pulmonary hypertension due to hypoxia than WT mice.[30] Although it is unknown whether there is a pathological state associated with a reduced production of AM, various cardiovascular diseases are associated with several-fold increases in circulating AM.[2,12,13] In TG mice, expression of AM in the aorta and kidney increased by 2- to 5-fold.[14] Therefore, increased AM in patients with hypertension and chronic renal failure may play a compensatory role with regard to blood pressure regulation. On the other hand, in septic shock in which the highest level of plasma AM was reported,[31,32] AM may be one of the factors contributing to hypotension. In the present study, compared with WT mice, TG mice showed 2-fold increase and KO mice about 50% decrease in AM. Thus, the AM levels in TG and KO mice were pathological rather than physiological. In iARF, AM KO mice subjected to ischemia/reperfusion had significantly higher serum urea nitrogen and creatinine levels than WT mice. Furthermore, histological analysis revealed that renal damage was significantly more severe in KO mice than in WT mice. These results suggest that high levels of AM may mitigate renal damage and decreases of AM below the physiological level may abrogate it.

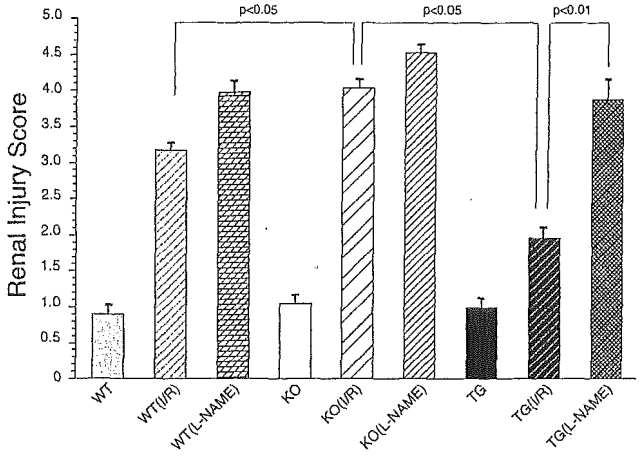

Figure 6. Effects of ischemia and preischemic treatment with L-NAME on renal injury scores in TG, WT, and KO mice. Values are means of 4 types of injury scores. (I/R) indicates ischemia/reperfusion; L-NAME, L-NAME+I/R.

Not only AM-induced vasodilation but also ACh-induced vasodilation was attenuated in AM TG mice. This mechanism is unclear from the present study; however, eNOS TG mice

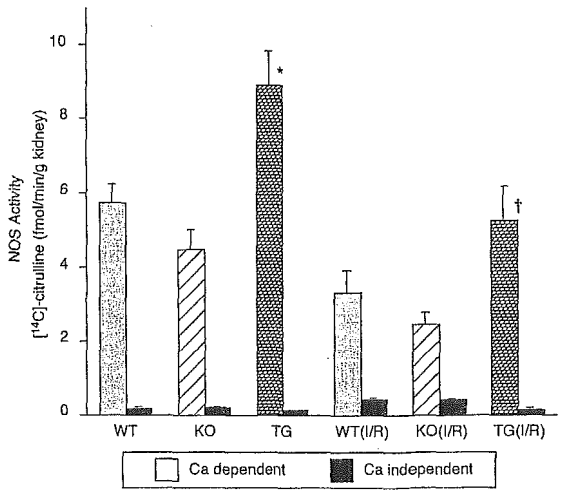

Figure 7. NO synthase activity in the kidneys of TG, WT, and KO mice. NO synthase activity was measured based on the conversion of L-arginine to L-citrulline. (I/R) indicates ischemia/reperfusion. *$P<0.05$ vs WT; †$P<0.05$ vs WT(I/R).

also showed hyporesponsiveness to endothelium-dependent vasodilators, but not to endothelium-independent vasodilators.[33] In these mice, the activity of soluble guanylate cyclase and the expression of cGMP-dependent protein kinase decreased, probably due to continuous activation of the NO-cGMP pathway.[34] A similar kind of downregulation of the signal transduction of the NO system may occur in AM TG mice. However, this mechanism may not totally explain the differences in vasodilatory responses of the 3 groups of mice because NO synthase inhibition increased RPP in AM TG mice to a greater extent. The responses to L-NMMA or E-4021 reflected the baseline NO releasing rates. The response of TG mice to NO may be attenuated. However, blood pressure and RPP in TG mice were still significantly lower, suggesting that the total vascular effects of endogenous NO in TG mice may overwhelm the attenuated response and be greater than those in WT mice at the baseline level. Thus, the differences in the responses to L-NMMA and E-4021 suggest the great differences in baseline NO release among the mice groups. On the other hand, when NO release was stimulated, nearly maximal renovasorelaxation in AM TG mice may at least in part explain the mechanism for attenuated vasodilatory responses to ACh. This is compatible with the findings of previous reports that L-NMMA caused greater vasoconstriction under increased NO release, including eNOS transgenic mice.[33,34]

In the present study, 24-hour reperfusion following 45-minute ischemia caused iARF in mice. Although many factors may involve renal injury caused by ischemia/reperfusion, the role of NO has been considered to be important; however, it is still controversial as to whether NO increases or decreases and as to which NO synthase is responsible for the change in NO in iARF. We have recently reported that tetrahydrobiopterin (BH4), a cofactor of NO synthase, of renal tissue is deficient in iARF and that replacement of BH4 restored renal endothelium-derived NO and improved renal injury in rats.[19] On the other hand, inhibition of NO synthesis by L-NAME aggravated renal injury. These findings suggest that endothelium-derived NO exerts cytoprotective effects in ischemia/reperfusion and its decrease enhances tissue injury. From this point of view, in TG mice the degree of renal injury and renal excretory dysfunction was less than in WT mice, suggesting that AM-induced NO release may contribute to mitigation of ischemic renal injury. In fact, renal NOS activity increased in AM TG mice. Pretreatment with L-NAME abolished the differences in renal function between TG mice and WT mice, supporting this possibility. It remains undetermined as to how NO mitigates ischemia/reperfusion injury. However, it is possible that NO is a potent antioxidant and traps superoxide during the reperfusion period. Furthermore, it has been reported that NO suppresses excessive increases in intracellular calcium by increasing cGMP.[35] NO-induced vasodilation also contributes to it. AM is reported to protect cultured endothelial cells from apoptosis and this effect is mediated by the stimulation of NO production by endothelial cells.[36]

From the results of L-NMMA administration and citrulline assay, we supposed that AM-induced renal protection might be exerted via NO release. The citrulline assay showed that the NOS activity was much lower in the renal cortex of all groups of mice than in the medulla. This finding was consistent with that of most previous studies, which found that NOS activity in the renal cortex was less than 10% of that in the medulla.[37–39] Because it is difficult to differentiate a calcium-dependent activity of NOS from a calcium-independent one, we did not analyze the small activity detected in the renal cortex. Although it is possible that NO released in the cortex may also work, it is suggested that NO derived from medullary vessels and tubuli would play a major role in protecting renal function.[40]

In conclusion, using genetically manipulated animals, we found that endogenous AM actually regulates renal vascular tone even by relatively small changes in its production. Furthermore, AM may exert a cytoprotective role in ischemic injury through its NO-releasing activity.

Acknowledgments

This study was supported in part by Grants-in-Aid Nos. 10218202, 13470141, and 13557061 from the Japanese Ministry of Education, Culture, Sports and Science. We thank Marie Morita, Reiko Sato, and Etsuko Taira for technical assistance.

References

1. Kitamura K, Kangawa K, Kawamoto M, Ichiki Y, Nakamura S, Matsuo H, Eto T. Adrenomedullin: a novel hypotensive peptide isolated from human pheochromocytoma. *Biochem Biophys Res Commun.* 1993;192:553–560.
2. Nishikimi T, Saito Y, Kitamura K, Ishimitsu T, Eto T, Kangawa K, Matsuo H, Omae T, Matsuoka H. Increased plasma levels of adrenomedullin in patients with heart failure. *J Am Coll Cardiol.* 1995;26:1424–1431.
3. Sugo S, Minamino N, Shoji H, Kangawa K, Kitamura K, Eto T, Matsuo H. Interleukin-1, tumor necrosis factor and lipopolysaccharide additively stimulate production of adrenomedullin in vascular smooth muscle cells. *Biochem Biophys Res Commun.* 1995;207:25–32.
4. Sugo S, Minamino N, Kangawa K, Miyamoto K, Kitamura K, Sakata J, Eto T, Matsuo H. Endothelial cells actively synthesize and secrete adrenomedullin [published erratum appears in *Biochem Biophys Res Commun* 1994;203:1363]. *Biochem Biophys Res Commun.* 1994;201:1160–1166.
5. Eguchi S, Hirata Y, Iwasaki H, Sato K, Watanabe TX, Inui T, Nakajima K, Sakakibara S, Marumo F. Structure-activity relationship of adrenomedullin, a novel vasodilatory peptide, in cultured rat vascular smooth muscle cells. *Endocrinology.* 1994;135:2454–2458.
6. Ishizaka Y, Tanaka M, Kitamura K, Kangawa K, Minamino N, Matsuo H, Eto T. Adrenomedullin stimulates cyclic AMP formation in rat vascular smooth muscle cells. *Biochem Biophys Res Commun.* 1994;200:642–646.
7. Shimekake Y, Nagata K, Ohta S, Kambayashi Y, Teraoka H, Kitamura K, Eto T, Kangawa K, Matsuo H. Adrenomedullin stimulates two signal transduction pathways, cAMP accumulation and Ca^{2+} mobilization, in bovine aortic endothelial cells. *J Biol Chem.* 1995;270:4412–4417.
8. Hirata Y, Hayakawa H, Suzuki Y, Suzuki E, Ikenouchi H, Kohmoto O, Kimura K, Kitamura K, Eto T, Kangawa K, et al. Mechanisms of adrenomedullin-induced vasodilation in the rat kidney. *Hypertension.* 1995;25:790–795.
9. Miura K, Ebara T, Okumura M, Matsuura T, Kim S, Yukimura T, Iwao H. Attenuation of adrenomedullin-induced renal vasodilatation by N^G-nitro L-arginine but not glibenclamide. *Br J Pharmacol.* 1995;115:917–924.
10. Majid DS, Kadowitz PJ, Coy DH, Navar LG. Renal responses to intra-arterial administration of adrenomedullin in dogs. *Am J Physiol.* 1996;270:F200–F205.
11. Hayakawa H, Hirata Y, Kakoki M, Suzuki Y, Nishimatsu H, Nagata D, Suzuki E, Kikuchi K, Nagano T, Kangawa K, Matsuo H, Sugimoto T, Omata M. Role of nitric oxide-cGMP pathway in adrenomedullin-induced vasodilation in the rat. *Hypertension.* 1999;33:689–695.

12. Ishimitsu T, Nishikimi T, Saito Y, Kitamura K, Eto T, Kangawa K, Matsuo H, Omae T, Matsuoka H. Plasma levels of adrenomedullin, a newly identified hypotensive peptide, in patients with hypertension and renal failure. *J Clin Invest.* 1994;94:2158–2161.
13. Jougasaki M, Wei CM, McKinley LJ, Burnett JC Jr. Elevation of circulating and ventricular adrenomedullin in human congestive heart failure. *Circulation.* 1995;92:286–289.
14. Shindo T, Kurihara H, Maemura K, Kurihara Y, Kuwaki T, Izumida T, Minamino N, Ju KH, Morita H, Oh-hashi Y, Kumada M, Kangawa K, Nagai R, Yazaki Y. Hypotension and resistance to lipopolysaccharide-induced shock in transgenic mice overexpressing adrenomedullin in their vasculature. *Circulation.* 2000;101:2309–2316.
15. Shindo T, Kurihara Y, Nishimatsu H, Moriyama N, Kakoki M, Wang Y, Imai Y, Ebihara A, Kuwaki T, Ju KH, Minamino N, Kangawa K, Ishikawa T, Fukuda M, Akimoto Y, Kawakami H, Imai T, Morita H, Yazaki Y, Nagai R, Hirata Y, Kurihara H. Vascular abnormalities and elevated blood pressure in mice lacking adrenomedullin gene. *Circulation.* 2001;104:1964–1971.
16. Chintala MS, Chiu PJ, Vemulapalli S, Watkins RW, Sybertz EJ. Inhibition of endothelial derived relaxing factor (EDRF) aggravates ischemic acute renal failure in anesthetized rats. *Naunyn Schmiedebergs Arch Pharmacol.* 1993;348:305–310.
17. Conger J, Robinette J, Villar A, Raij L, Shultz P. Increased nitric oxide synthase activity despite lack of response to endothelium-dependent vasodilators in postischemic acute renal failure in rats. *J Clin Invest.* 1995; 96:631–638.
18. Noiri E, Peresleni T, Miller F, Goligorsky MS. In vivo targeting of inducible NO synthase with oligodeoxynucleotides protects rat kidney against ischemia. *J Clin Invest.* 1996;97:2377–2383.
19. Kakoki M, Hirata Y, Hayakawa H, Suzuki E, Nagata D, Tojo A, Nishimatsu H, Nakanishi N, Hattori Y, Kikuchi K, Nagano T, Omata M. Effects of tetrahydrobiopterin on endothelial dysfunction in rats with ischemic acute renal failure. *J Am Soc Nephrol.* 2000;11:301–309.
20. Ichiki Y, Kitamura K, Kangawa K, Kawamoto M, Matsuo H, Eto T. Distribution and characterization of immunoreactive adrenomedullin in human tissue and plasma. *FEBS Lett.* 1994;338:6–10.
21. Hayakawa H, Hirata Y, Suzuki E, Sugimoto T, Matsuoka H, Kikuchi K, Nagano T, Hirobe M. Mechanisms for altered endothelium-dependent vasorelaxation in isolated kidneys from experimental hypertensive rats. *Am J Physiol.* 1993;264:H1535–H1541.
22. Hirata Y, Hayakawa H, Suzuki E, Kimura K, Kikuchi K, Nagano T, Hirobe M, Omata M. Direct measurements of endothelium-derived nitric oxide release by stimulation of endothelin receptors in rat kidney and its alteration in salt-induced hypertension. *Circulation.* 1995;91:1229–1235.
23. Saeki T, Adachi H, Takase Y, Yoshitake S, Souda S, Saito I. A selective type V phosphodiesterase inhibitor, E4021, dilates porcine large coronary artery. *J Pharmacol Exp Ther.* 1995;272:825–831.
24. Solez K, Morel-Maroger L, Sraer JD. The morphology of "acute tubular necrosis" in man: analysis of 57 renal biopsies and a comparison with the glycerol model. *Medicine.* 1979;58:362–376.
25. Kurihara Y, Kurihara H, Suzuki H, Kodama T, Maemura K, Nagai R, Oda H, Kuwaki T, Cao WH, Kamada N, et al. Elevated blood pressure and craniofacial abnormalities in mice deficient in endothelin-1. *Nature.* 1994;368:703–710.
26. Huang PL, Huang Z, Mashimo H, Bloch KD, Moskowitz MA, Bevan JA, Fishman MC. Hypertension in mice lacking the gene for endothelial nitric oxide synthase. *Nature.* 1995;377:239–242.
27. Nuki C, Kawasaki H, Kitamura K, Takenaga M, Kangawa K, Eto T, Wada A. Vasodilator effect of adrenomedullin and calcitonin gene-related peptide receptors in rat mesenteric vascular beds. *Biochem Biophys Res Commun.* 1993;196:245–251.
28. Watanabe TX, Itahara Y, Inui T, Yoshizawa-Kumagaye K, Nakajima K, Sakakibara S. Vasopressor activities of N-terminal fragments of adrenomedullin in anesthetized rat. *Biochem Biophys Res Commun.* 1996; 219:59–63.
29. Shesely EG, Maeda N, Kim HS, Desai KM, Krege JH, Laubach VE, Sherman PA, Sessa WC, Smithies O. Elevated blood pressures in mice lacking endothelial nitric oxide synthase. *Proc Natl Acad Sci U S A.* 1996;93:13176–13181.
30. Fagan KA, Fouty BW, Tyler RC, Morris KG Jr, Hepler LK, Sato K, LeCras TD, Abman SH, Weinberger HD, Huang PL, McMurtry IF, Rodman DM. The pulmonary circulation of homozygous or heterozygous eNOS-null mice is hyperresponsive to mild hypoxia. *J Clin Invest.* 1999; 103:291–299.
31. Hirata Y, Mitaka C, Sato K, Nagura T, Tsunoda Y, Amaha K, Marumo F. Increased circulating adrenomedullin, a novel vasodilatory peptide, in sepsis. *J Clin Endocrinol Metab.* 1996;81:1449–1453.
32. Nishio K, Akai Y, Murao Y, Doi N, Ueda S, Tabuse H, Miyamoto S, Dohi K, Minamino N, Shoji H, Kitamura K, Kangawa K, Matsuo H. Increased plasma concentrations of adrenomedullin correlate with relaxation of vascular tone in patients with septic shock. *Crit Care Med.* 1997;25:953–957.
33. Ohashi Y, Kawashima S, Hirata K, Yamashita T, Ishida T, Inoue N, Sakoda T, Kurihara H, Yazaki Y, Yokoyama M. Hypotension and reduced nitric oxide-elicited vasorelaxation in transgenic mice overexpressing endothelial nitric oxide synthase. *J Clin Invest.* 1998;102: 2061–2071.
34. Yamashita T, Kawashima S, Ohashi Y, Ozaki M, Rikitake Y, Inoue N, Hirata K, Akita H, Yokoyama M. Mechanisms of reduced nitric oxide/cGMP-mediated vasorelaxation in transgenic mice overexpressing endothelial nitric oxide synthase. *Hypertension.* 2000;36:97–102.
35. Conger JD, Robinette JB, Schrier RW. Smooth muscle calcium and endothelium-derived relaxing factor in the abnormal vascular responses of acute renal failure. *J Clin Invest.* 1988;82:532–537.
36. Sata M, Kakoki M, Nagata D, Nishimatsu H, Suzuki E, Aoyagi T, Sugiura S, Kojima H, Nagano T, Kangawa K, Matsuo H, Omata M, Nagai R, Hirata Y. Adrenomedullin and nitric oxide inhibit human endothelial cell apoptosis via a cyclic GMP-independent mechanism. *Hypertension.* 2000;36:83–88.
37. Nava E, Llinas MT, Gonzalez JD, Salazar FJ. Nitric oxide synthase activity in renal cortex and medulla of normotensive and spontaneously hypertensive rats. *Am J Hypertens.* 1996;9:1236–1239.
38. Hayakawa H, Raij L. Nitric oxide synthase activity and renal injury in genetic hypertension. *Hypertension.* 1998;31:266–270.
39. Wu F, Park F, Cowley AW Jr, Mattson DL. Quantification of nitric oxide synthase activity in microdissected segments of the rat kidney. *Am J Physiol.* 1999;276:F874–F881.
40. Szentivanyi M Jr, Zou AP, Maeda CY, Mattson DL, Cowley AW Jr. Increase in renal medullary nitric oxide synthase activity protects from norepinephrine-induced hypertension. *Hypertension.* 2000;35:418–423.

J Mol Med (2002) 80:105–116
DOI 10.1007/s00109-001-0284-4

ORIGINAL ARTICLE

T. Shindo · H. Kurihara · K. Maemura · Y. Kurihara
O. Ueda · H. Suzuki · T. Kuwaki · K.-H. Ju · Y. Wang
A. Ebihara · H. Nishimatsu · N. Moriyama
M. Fukuda · Y. Akimoto · H. Hirano · H. Morita
M. Kumada · Y. Yazaki · R. Nagai · K. Kimura

Renal damage and salt-dependent hypertension in aged transgenic mice overexpressing endothelin-1

Received: 28 June 2001 / Accepted: 28 August 2001 / Published online: 8 November 2001

H. Kurihara (✉)
Division of Integrative Cell Biology, Department of Embryogenesis, Institute of Molecular Embryology and Genetics, Kumamoto University, 2-2-1 Honjo, Kumamoto 860–0811, Japan
e-mail: kurihara@kaiju.medic.kumamoto-u.ac.jp
Tel.: +81-96-3736615, Fax: +81-96-3736618

T. Shindo · K. Maemura · Y. Kurihara · Y. Wang · H. Morita · R. Nagai
Department of Cardiovascular Medicine, Graduate School of Medicine, University of Tokyo, Tokyo, Japan

H. Kurihara
Department of Embryogenesis, Institute of Molecular Embryology and Genetics, Kumamoto University, Kumamoto, Japan

O. Ueda
Chugai Pharmaceutical Corporation, Shizuoka, Japan

H. Suzuki
National Research Center for Protozoan Diseases, Obihiro University of Agriculture and Veterinary Medicine, Obihiro, Japan

T. Kuwaki
Department of Physiology, School of Medicine, Chiba University, Chiba, Japan

K.-H. Ju
Department of Physiology, Graduate School of Medicine, University of Tokyo, Tokyo, Japan

A. Ebihara
The Institute for Adult Disease Asahi Life Foundation, Tokyo, Japan

H. Nishimatsu · N. Moriyama
Department of Urology, Graduate School of Medicine, University of Tokyo, Tokyo, Japan

M. Fukuda · Y. Akimoto · H. Hirano
Department of Anatomy, Kyorin University, Tokyo, Japan

M. Kumada
St Luke's College of Nursing, Tokyo, Japan

Y. Yazaki
The Hospital International Medical Center of Japan, Tokyo, Japan

K. Kimura
Department of Nephrology and Endocrinology, Graduate School of Medicine, University of Tokyo, Tokyo, Japan

K. Kimura
Division of Nephrology and Hypertension, Department of Internal Medicine, St. Marianna University School of Medicine, Kanagawa, Japan

J Mol Med 2002 Feb;80(2):69–70

Comment on:

- J Mol Med. 2002 Feb;80(2):105–16.

Endothelin, nephropathy, and blood pressure.

Luft FC.

Franz-Volhard-Klinik, Humboldt University of Berlin, Wiltbergstrass 50, 13125 Berlin-Buch, Germany. luft@fvk-berlin.de

TAKAYUKI SHINDO received his PhD in cardiology from the University of Tokyo, Tokyo, Japan. He is presently a Research Fellow of the Organization for Drug ADR Relief, R&D Promotion and Product Review of Japan. His research interests include the pathophysiological assessment of cardiovascular disease by the mice gene-engineering approach.

KENJIRO KIMURA received his PhD in nephrology from the University of Tokyo, Tokyo, Japan. He is presently Professor of Medicine, Director of Division of Nephrology and Hypertension at St. Marianna University School of Medicine. His research interests include the pathogenesis of renal disease and the mechanisms for progression of renal diseases.

Abstract The recent development of endothelin-1 (ET-1) antagonists and their potential use in the treatment of human disease raises questions as to the role of ET-1 in the pathophysiology of such cardiovascular ailments as hypertension, heart failure, renal failure and atherosclerosis. It is still unclear, for example, whether activation of an endogenous ET-1 system is itself the primary cause of any of these ailments. In that context, the phenotypic manifestations of chronic ET-1 overproduction may provide clues about the tissues and systems affected by ET-1. We therefore established two lines of transgenic mice overexpressing the ET-1 gene under the direction of its own promoter. These mice exhibited low body weight, diminished fur density and two- to fourfold increases in

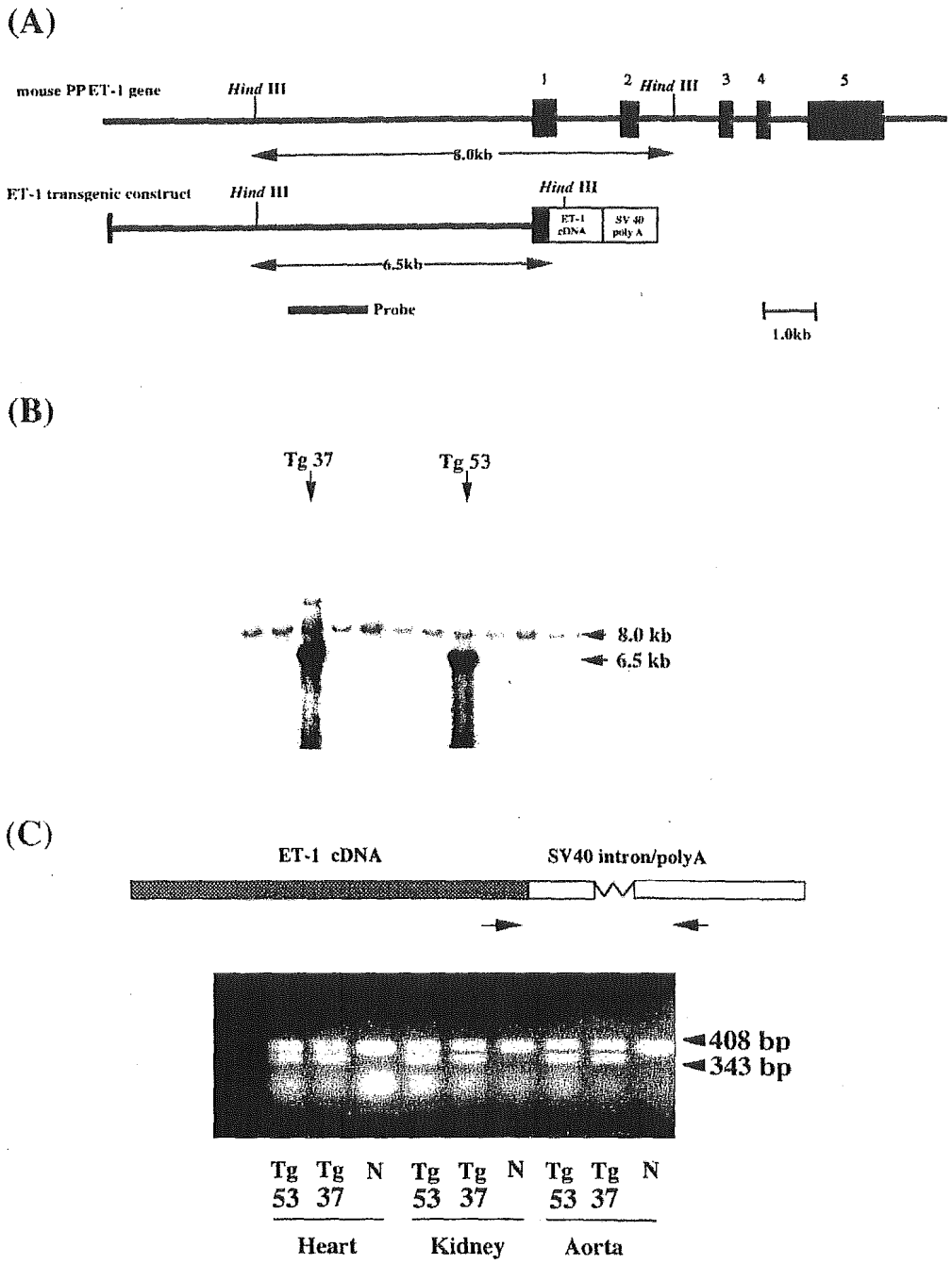

Fig. 1 A Structure and restriction maps of the mouse PPET-1 gene and the transgenic construct. *Filled boxes* represent exons 1–5 of the PPET-1 gene. The length of the *Hind*III-digested diagnostic DNA fragments and the probe for Southern blot analysis are shown. **B** Representative genomic Southern blot analysis. The 8.0-kb and 6.5-kb *Hind*III bands reflect the authentic PPET-1 gene and the transgene, respectively. **C** Representative RT-PCR demonstrating expression of the ET-1 transgene. *Arrows* in the figure indicate the primers for RT-PCR. In Tg 37 and Tg 53, the amplified products derived from the integrated transgene could be discriminated by a 65-bp difference caused by the SV40 intron, whereas no such product was detected in the nonexpresser (*N*). **D** Plasma and tissue endothelin-1 (*ET-1*) concentrations in ET-1 transgenic and wild-type mice. $^{\#}P<0.05$, $^{*}P<0.01$ versus wild-type mice. **E, F** Representative sections showing immunohistochemical staining for ET-1 in the kidneys of wild-type (**E**) and Tg 53 transgenic (**F**) mice. Specific staining for ET-1 was detected in the glomeruli (*g*) and vascular endothelium (*a*) of transgenic mice, whereas wild-type kidneys showed only faint staining in glomeruli. *Scale bars* in **E** and **F**, 100 μm

the ET-1 levels measured in plasma, heart, kidney and aorta. There were no apparent histological abnormalities in the visceral organs of young (8 weeks old) transgenic mice, nor was their blood pressure elevated. In aged (12 months old) transgenic mice, however, renal manifestations, including prominent interstitial fibrosis, renal cysts, glomerulosclerosis and narrowing of arterioles, were detected. These pathological changes were accompanied by decreased creatinine clearance, elevated urinary protein excretion and salt-dependent hypertension. It thus appears that mild, chronic overproduction of ET-1 does not primarily cause hypertension but triggers damaging changes in the kidney which lead to the susceptibility to salt-induced hypertension.

Keywords Aging · Blood pressure · Endothelin · Hypertension · Renal function

Since its initial characterization as an endothelial cell-derived vasoconstrictor a decade ago [1], the peptide endothelin-1 (ET-1) has been found to possess a diverse set of biological activities, including effects on cell proliferation and hypertrophy, regulation of hormone release and modulation of central nervous system activity [2, 3, 4]. In addition, elevated plasma ET-1 has been associated with such cardiovascular diseases as hypertension [5], heart failure [6], renal failure [7] and atherosclerosis [8], thus implicating it in the regulation of cardiovascular ho-

Fig. 1D–F

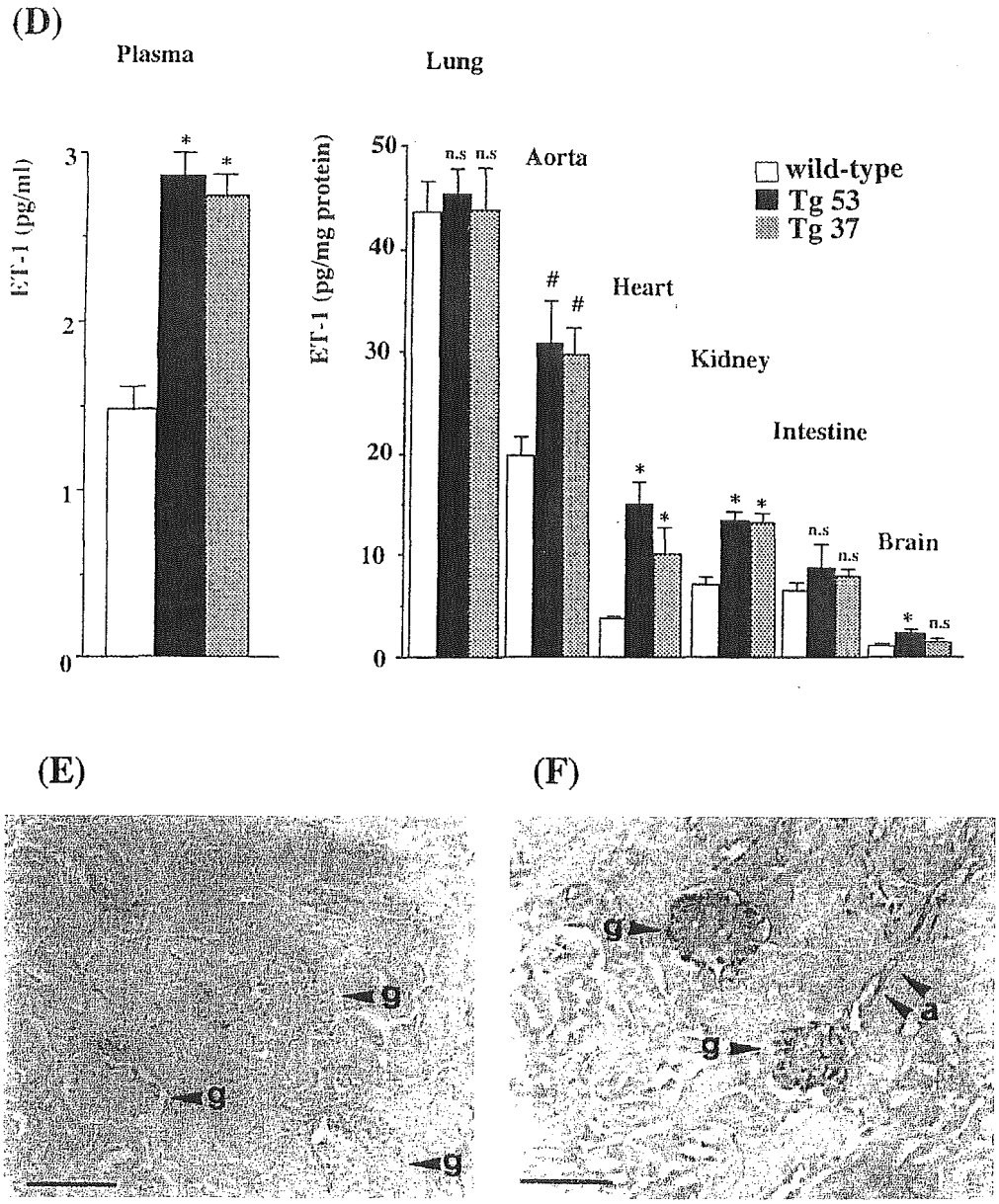

meostasis. The recent development of selective ET antagonists and their potential use in the treatment of cardiovascular disease raises questions as to the role of ET-1 in the disease process [9]. It is still unclear whether activation of an endogenous ET-1system could be the primary cause of any of the aforementioned ailments. For example, patients with essential hypertension had elevated plasma ET-1 levels, but there was no significant correlation between the plasma ET-1 level and systolic or diastolic blood pressure (BP) in these patients [10].

Animal models in which ET-1 production is chronically increased should serve as a useful tool with which to obtain a better understanding of the function of ET-1 in cardiovascular pathophysiology. In particular, the use of transgenic mice overexpressing ET-1 enables us to focus on the effects of chronically elevated ET-1 on selected organs, so as to better understand the specific benefits of anti-ET therapy. Based on our previous work showing the utility of the murine (prepro)endothelin-1 (PPET-1) gene 5′-flanking region for this purpose [11], we generated transgenic mice using a DNA construct in which the promoter region was inserted upstream of murine ET-1 cDNA and analyzed their phenotype with special reference to BP regulation and organ damage.

Materials and methods

Transgenic construct

A mouse ET-1 cDNA fragment encompassing the open reading frame was obtained from mouse lung cDNA by reverse transcription (RT) polymerase chain reaction (PCR) using primers deduced from the previously reported sequence [12]. The amplified 1.0-kb fragment was cloned into pCRII vector using a TA cloning kit (Invitrogen), and *Not*I sites were placed at either end of the fragment

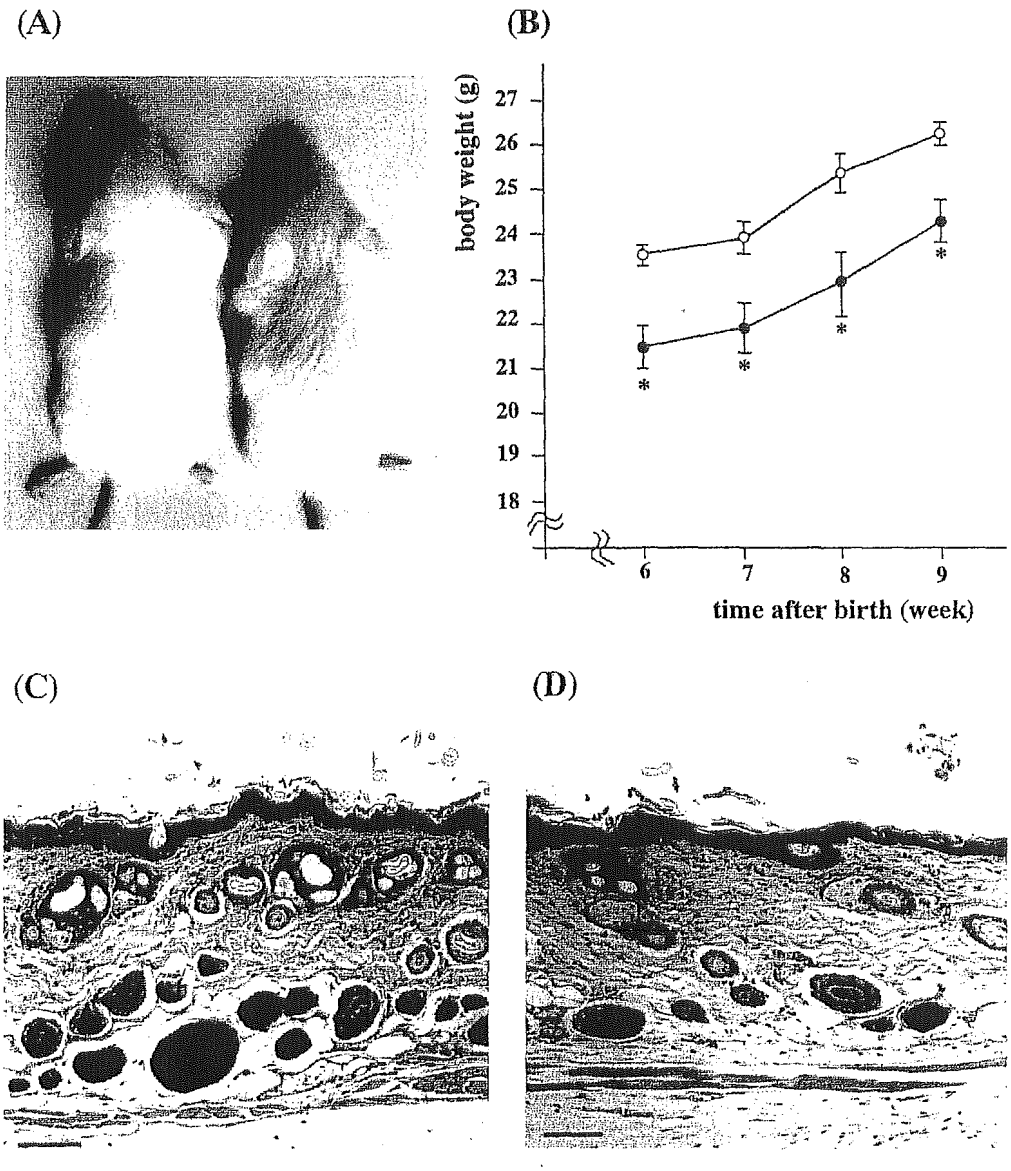

Fig. 2 **A** Representative specimens of 10-week-old transgenic (*right*) and wild-type (*left*) mice. Note the smaller size of the transgenic mouse and the courser, sparser fur. **B** Time-dependent increases in body weight in transgenic (*closed circles*) and wild-type (*open circles*) mice (n=10 for each). $^{*}P<0.01$ versus wild-type mice. **C**, **D** Representative skin sections from wild-type (**C**) and transgenic (**D**) mice. *Scale bars* in **C** and **D**, 200 μm

using synthetic linkers. The resultant *Not*I cassette was then inserted into a plasmid containing a 9.2-kb fragment of the murine PPET-1 gene 5′-flanking region, including a 131-bp sequence from exon 1 and a 0.7-kb SV40-derived sequence with an intron and an additional poly-A signal [11]. The final construct is illustrated in Fig. 1A.

Generation and identification of transgenic mice

The investigation conforms with the *Guide for the Care and Use of Laboratory Animals* published by the US National Institutes of Health (NIH Publication No. 85–23, revised 1996).

The PPET-1 5′-flanking promoter region-ET-1 cDNA construct was liberated from the vector by *Xho*I digestion and then purified using agarose gel electrophoresis and a Geneclean kit (BIO101). The purified DNA was dissolved in 5 mM Tris (pH 7.4) plus 0.1 mM EDTA before pronuclear injection into donor eggs prepared from FvB mice. The final injection concentration was calculated to be 500 copies/pl. Microinjected eggs were transferred to the oviducts of pseudopregnant ICR foster mothers and allowed to develop to term. Founder mice were identified by standard Southern blot analysis of tail DNA using a 2-kb fragment of the PPET-1 promoter gene sequence as a probe. When the genomic DNA was digested with *Hin*dIII, a 6.5-kb transgene band, distinguishable from the 8.0-kb authentic gene band, was observed.

For RT-PCR, the sense primer (5′-TAGGGAGTGTTCGTGTCTGACTCA-3′) was chosen within the mouse ET-1 cDNA sequence. The antisense primer (5′-AGATGGCATTTCTTCTGAGC-3′) was chosen within an SV40 intron/poly-A additional signal sequence. These primers were chosen to be situated upstream and downstream of the SV40 intron sequence, respectively. In transgenic mice that showed the transcription of the transgene, the RT-PCR product from the mRNA was 65 bp shorter because of the splicing at the SV40 intron site (Fig. 1C).

Endothelin-1 measurement

ET-1 was extracted from tissue and plasma as described previously [13, 14]. Immunoreactive ET-1 was measured using a commercial endothelin enzyme immunoassay kit according to the manufacturer's (Wako) instructions.

Immunohistochemistry

Samples embedded in OCT compound were cut into 8-μm frozen sections on a cryostat. Slide-mounted tissue sections were washed

with PBS, treated with 0.3% H_2O_2 in methanol, preincubated with goat nonimmune serum, and then incubated for 16 h at 4°C with rabbit anti-rat polyclonal ET-1 antibody. Thereafter, the sections were incubated for 60 min at 37°C with biotinylated goat anti-rabbit IgG, washed, treated with avidin-biotinylated horseradish peroxidase complex (Vectastain ABC kit, Vector), and developed in 0.004% H_2O_2 and 0.02% diaminobenzidine tetrahydrochloride. Samples labeled with preimmune serum instead of the primary antibody served as a negative control.

Electron microscopy

Small samples of the specimens were fixed with glutaraldehyde and osmium tetroxide, embedded in Epon (Epok) 812 (Oken Shoji, Tokyo, Japan), cut into 0.1-μm sections, double-stained with uranyl acetate or phosphotungstic acid and lead citrate, and examined with an electron microscope.

Vascular casting and scanning electron microscopy

Mice were anesthetized with sodium pentobarbital, and the aorta was cannulated via the left ventricle and perfused with 100 ml PBS containing 0.1% heparin. The lower portion of the descending aorta was then cross-clamped, and perfusion fixation was carried out for 5 min using 100 ml of 2.5% glutaraldehyde at 37°C. Thereafter, 10 ml of casting resin (Mercox CL2B, Dainippon-ink and Chemical, Tokyo, Japan), mixed with a polymerizer in a 1.7% volume ratio, was infused under hand pressure and allowed to polymerize for 30 min at room temperature. The kidneys were then removed and immersed in a 20% KOH solution at room temperature for 1–2 days to corrode the tissue. After washing in water, the vascular casts were dried in an incubator at 40°C. Areas of the cast corresponding to the cortex were then cut with a razor blade into small pieces suitable for observation, gold-coated with an ion sputter and observed under a scanning electron microscope (JSM-5600LV, JEOL, Tokyo, Japan) using an accelerating voltage of 15 kV.

Measurement of blood pressure

Male transgenic mice heterozygous for the ET-1 transgene and their wild-type littermates were maintained on normal mouse chow containing 1% NaCl. Using a ventilator (Harvard rodent ventilator model 683), the mice were then halothane anesthetized, and their femoral arteries were cannulated with polyethylene tubing (I.D., 0.28 mm; O.D., 0.61 mm). To measure BP, the cannula was connected a pressure transducer (TP-400T, Nihon-Kohden), and arterial pressure was determined every 2.5 s using a peak detector (AP-611G, Nihon-Kohden). Pulsatile BP was monitored in this way for more than 5 h while the mice were conscious and unrestrained within a quiet environment. BP data were stored on tape along with the corresponding heart rates, which were computed using a tachometer (AT-601G, Nihon-Kohden). The data were then input to a computer, and the mean values for each variable were calculated for 2-h segments composed of 2880 sample points each.

To investigate the salt sensitivity of the mice, diet containing a high (8%) amount of sodium was provided for up to 3 weeks. This dose could cause BP elevation in Dahl salt-sensitive rats within 3 weeks [15]. The systolic BP was measured by a programmable sphygmomanometer connected to a cuff probe for mice (98A, Softron). Unanesthetized mice were introduced into a small holder and placed within a thermostatically controlled warming drum and maintained at 37°C during the measurements.

Evaluation of renal function

All mice were housed in individual metabolic cages, and a series of 24-h urine sample collections were made for 5 days. In each mouse, we used the urine samples from days 3–5 and calculated the mean urine volume and concentrations of urinary protein and creatinine. After 5 days, blood was drawn to measure serum creatinine. Creatinine clearance was used as an index of glomerular filtration rate and was calculated using the formula: creatinine clearance=urinary creatinine × urine volume/serum creatinine.

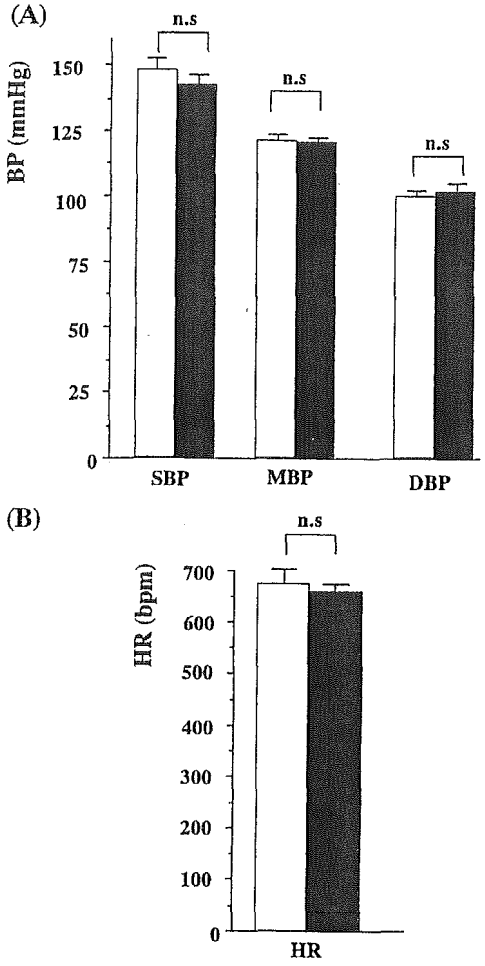

Fig. 3 Comparison of basal arterial blood pressure (BP) (**A**) and heart rates (**B**) in conscious, unrestrained ET-1 transgenic mice (n=8, *filled columns*) and their wild-type littermates (n=10, *open column*). (*DBP* Diastolic blood pressure, *HR* heart rate, *MBP* mean blood pressure, *SBP* systolic blood pressure)

Statistical analysis

Data are expressed as means ±SEM. Student's t-test was used to evaluate differences between groups. Values of $P<0.05$ were considered significant.

Results

Establishment and characterization of ET-1 transgenic mice

Microinjection of the transgenic construct into fertilized mouse eggs gave rise to 50 live-born offspring. Among them, eight were founders carrying the transgene, which was identified by Southern blot analysis of the genomic DNA (Fig. 1B). Amplification of the products by RT-

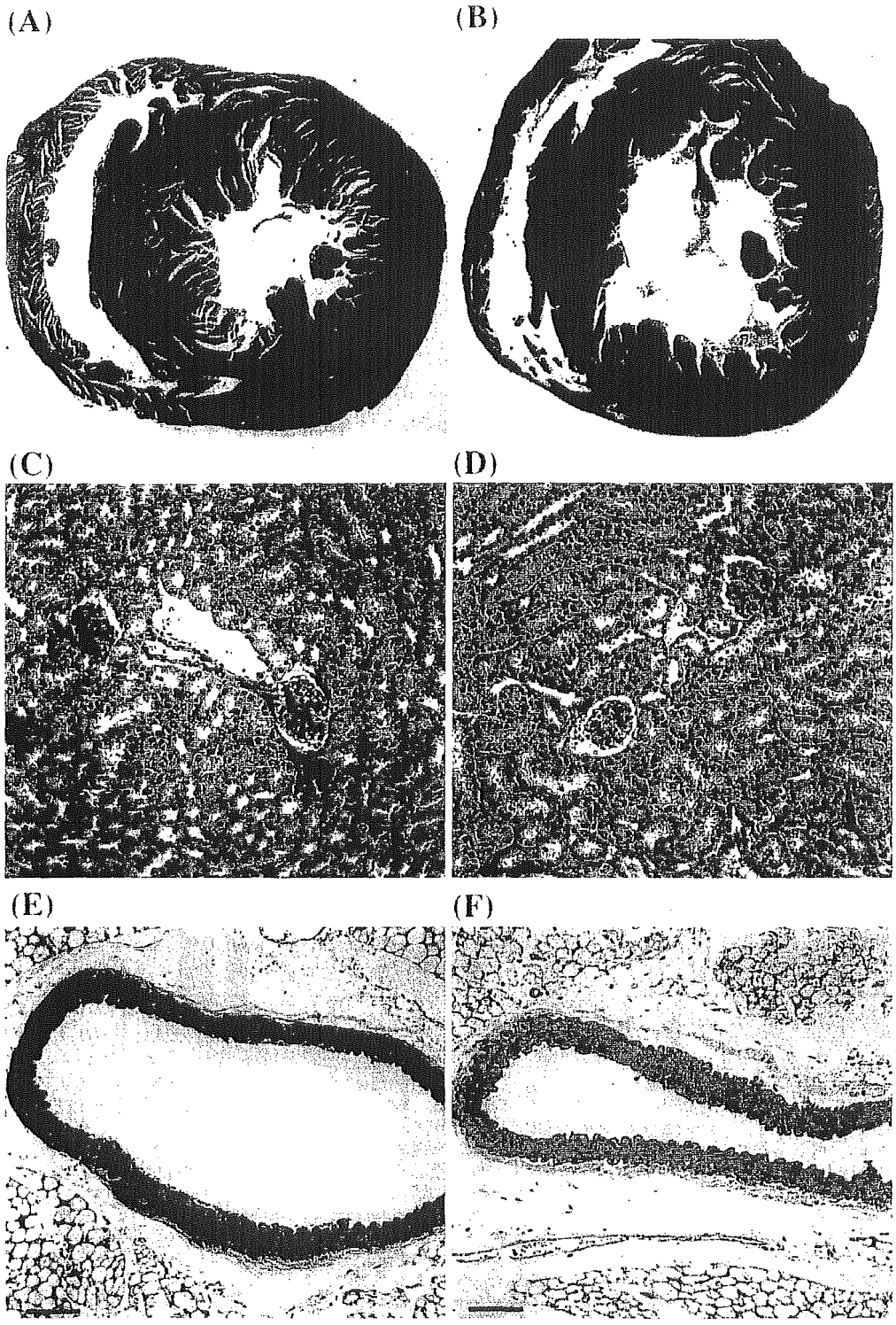

Fig. 4 Representative sections showing histological characteristics of the heart (**A**, **B**), kidney (**C**, **D**) and aorta (**E**, **F**) from 8- to 10-week-old wild-type (**A**, **C**, **E**) and ET-1 transgenic (**B**, **D**, **F**) mice. *Scale bars* in **C** and **D**, 100 μm; **E** and **F**, 200 μm

PCR confirmed that two lines transcribed the transgene (Fig. 1C). The two lines, designated Tg 53 and Tg 37, carried ten and nine copies of the transgene, respectively. As compared to their wild-type littermates, ET-1 concentrations in the plasma, aorta, heart, kidney and intestine were elevated about twofold in both lines (Fig. 1D). The effect of ET-1 overexpression was assessed mainly using the Tg 53 line in the latter studies, because the expression levels in each organ were almost equal and histological changes were identical between these lines.

Localization of ET-1 expression in the kidney was analyzed immunohistochemically. The glomeruli in kidney samples from transgenic mice were intensively labeled by anti-ET-1 antibody (Fig. 1F), whereas the signal from kidneys of wild-type mice was small (Fig. 1E). This pat-

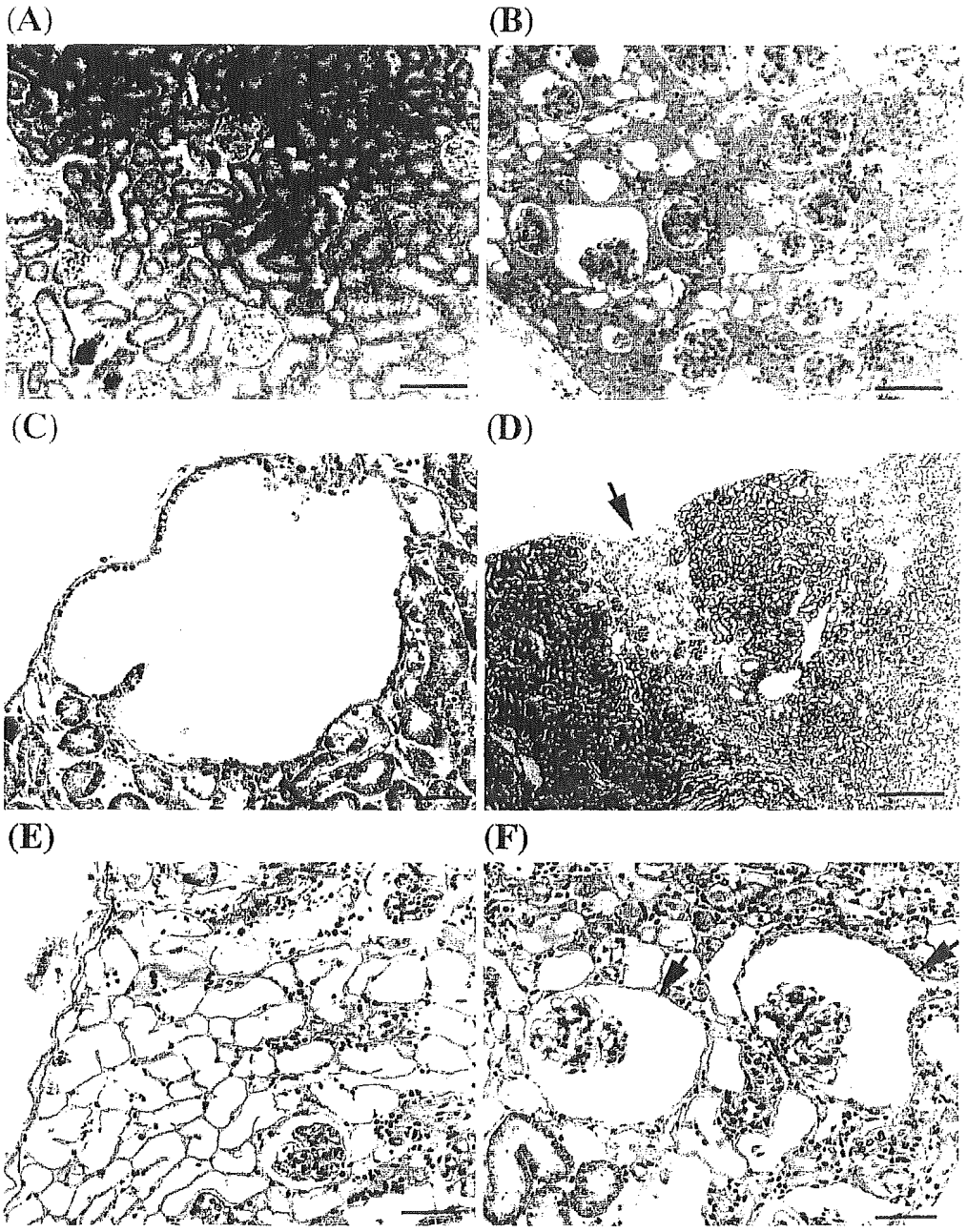

Fig. 5 Kidney sections from 12-month-old wild-type (**A**) and transgenic (**B–F**) mice. Interstitial fibrosis in transgenic mice was made apparent by staining blue with Masson Trichrome stain (**B**). **C–F** Cystic lesions detected in the kidney of transgenic mice. **C** Enlarged renal cyst located at the surface of the kidney. **D, E** Focal assembly of small cysts. **F** Glomerular cysts; note the abnormal dilatation of Bowman's capsule (*arrows*) and the shrinkage of the glomerular tuft. **G–J** Glomeruli from transgenic (**H, J**) and wild-type (**G, I**) mice, **G, H** PAS stain, **I, J** immunohistochemistry of fibronectin. Glomeruli of transgenic mice exhibited increased numbers of mesangial cells, the accumulation of mesangial matrix and thickening of the basement membrane (**H**). Immunohistochemistry of fibronectin revealed strong positive staining in the mesangial area in transgenic mice (**J**). *Scale bars* in **A** and **B**, 100 μm; **C, E** and **F** 50 μm; **D** 20 μm; and **G–J** 200 μm. **K** Comparison of glomerular planar area in wild-type (*open column*) and transgenic mice (*filled column*). $^{*}P<0.01$ versus wild-type mice

tern of ET-1 expression in the kidney was almost identical to that in PPET-1-luciferase transgenic mice exhibiting vasculature-selective transgene expression driven by the same promoter [11].

Appearance of ET-1 transgenic mice

Transgenic mice weighed about 90% as much as their wild-type littermates at every stage examined (Fig. 2A, B). In fact, the reduced body weight was already apparent at birth, when the weight of the fat between the scapulae was also only about 90% that of the wild-type mice. In addition, the fur of the transgenic mice was coarse, and the number of follicles present in skin sections was diminished (Fig. 2C, D). In all other respects, the appearance, behavior and fertility of the transgenic lines were unaffected.

Measurement of blood pressure, heart rate and creatinine clearance in young mice

When the arterial BP was assessed in 8- to 10-week-old, conscious, unrestrained mice, no significant differences between wild-type (n=10) and transgenic (n=8) mice were found (mean BP, 121±1 mmHg versus 120±2 mmHg; heart rate, 674±26 bpm versus

Fig. 5G–K Legend see page 111

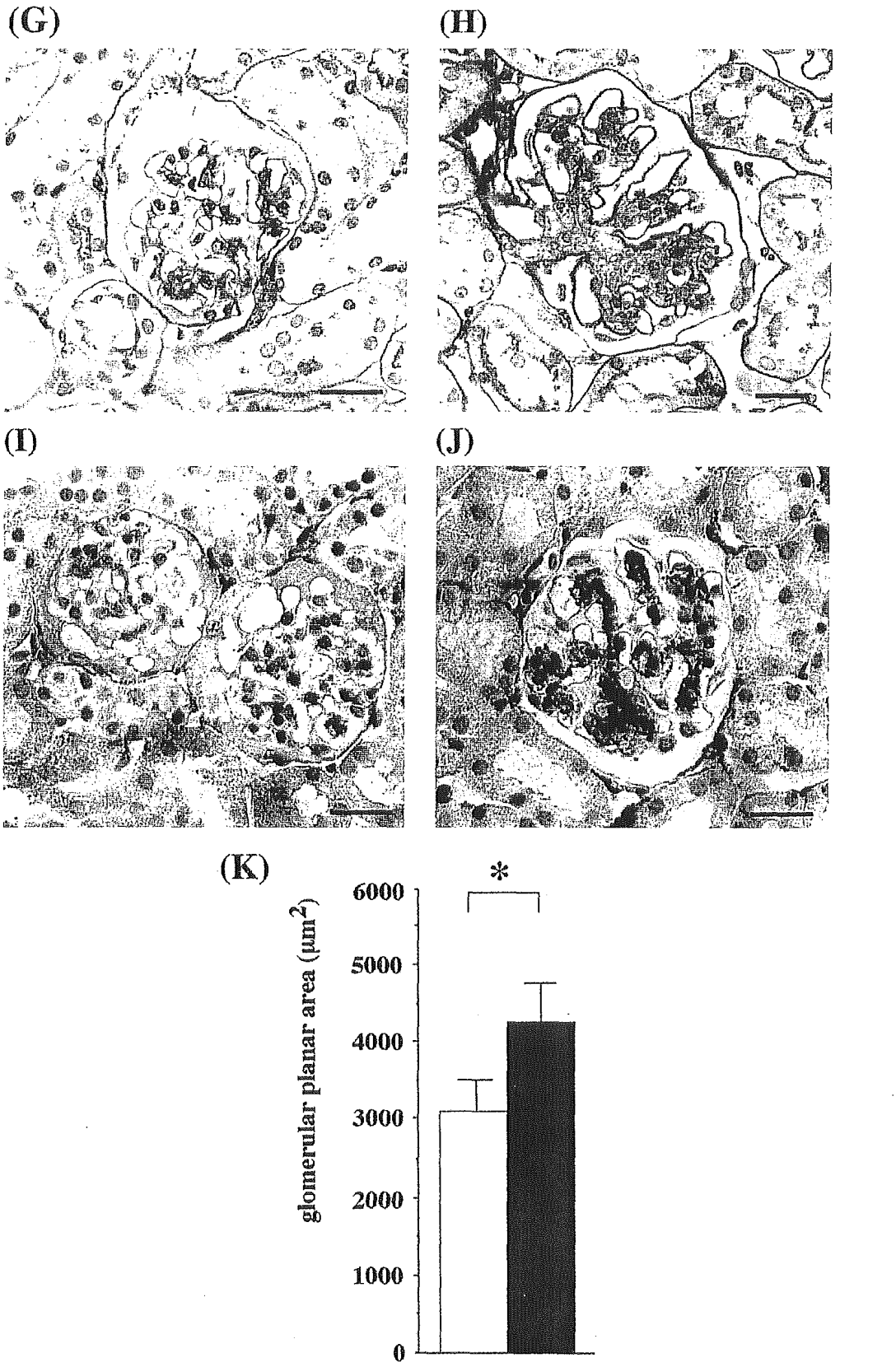

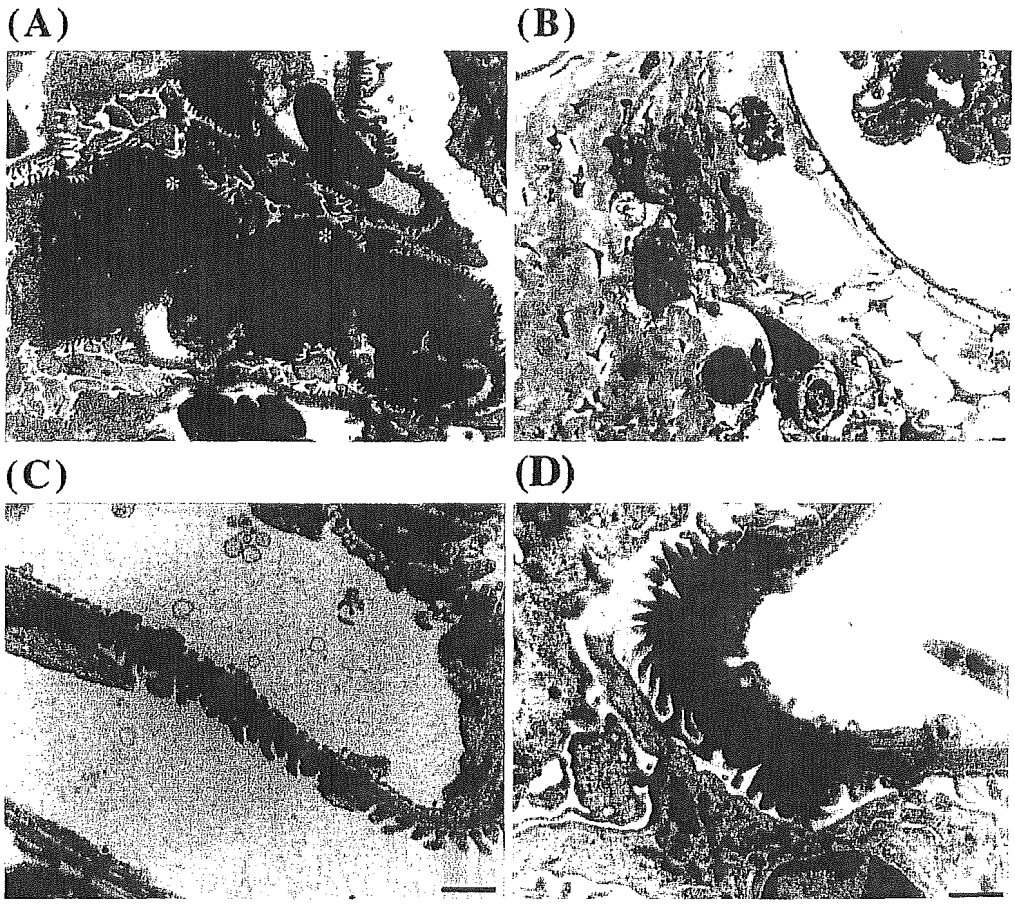

Fig. 6 Electron microscopic examination of transgenic (**A**, **B**, **D**) and wild-type (**C**) mice. *Asterisks* indicate increased mesangial matrix (**A**) or hyalinization of the interstitium (**B**). **D** *Arrowheads* indicate thickening of the basement membrane in transgenic mice. *Scale bars* in **A**, **C** and **D** 1 μm; **B** 2 μm

660±13 bpm) (Fig. 3A, B). In addition, there was no significant difference in the creatinine clearance between these mice. (wild-type: 5.1±0.4 ml·min^{-1}·kg^{-1}, transgenic: 5.0±0.3 ml·min^{-1}·kg^{-1}, n=7 in each).

Histological examination of young mice

Histological examination of the hearts (Fig. 4A, B), kidneys (Fig. 4C, D) and aortas (Fig. 4E, F) of 8- to 10-week-old ET-1 transgenic and wild-type mice revealed no apparent lesions in the transgenic mice. In particular, neither atherosclerosis of the aortic wall nor cardiac hypertrophy was noted.

Histological examination of aged mice

When aged (12 months old) transgenic mice of Tg 53 and Tg 37 were later examined, cardiac hypertrophy and atherosclerotic lesions of the aortic wall were still not detected (data not shown); however, prominent changes were found in the kidney in both lines. Numerous cystic lesions were detected in the aged transgenic mice, as were areas of focal interstitial fibrosis (Fig. 5B). The cystic lesions could be classified into three types: (1) renal cysts (planar area, 110,320±2984 μm^2) derived from the occlusion and dilatation of urinary tubules (Fig. 5C); (2) focal assemblies of small cysts (planar area, 819±104 μm^2), which were mainly observed in areas containing pronounced interstitial fibrosis, forming a wedge-shaped distribution at the renal cortex (Fig. 5D, E); and (3) glomerular cysts (planar area, 12,152±924 μm^2) (Fig. 5F). Some of the Bowman's capsules showed abnormal dilatation, and that the glomerular tufts of such glomeruli were shrunken. Comparison of the glomeruli of transgenic and wild-type mice also revealed increased numbers of mesangial cells and the accumulation of mesangial matrix in transgenic mice (Fig. 5H) and glomerular planar areas were significantly larger in transgenic mice (wild-type, 3095±450 μm^2; transgenic, 4240±486 μm^2, P<0.01) (Fig. 5K). In addition, PAS staining showed the basement membranes of the glomeruli from transgenic mice to be thickened and wrinkled (Fig. 5H). Immunohistochemistry of fibronectin revealed strong positive staining in the mesangial area of the glomeruli from transgenic mice (Fig. 5J), whereas no staining was detected in wild-type mice (Fig. 5I).

Electron microscopic examinations

The presence of increased mesangial matrix in the glomeruli and hyalinization of the interstitium of transgenic mice were confirmed by electron microscopy (Fig. 6A, B), as was the partial thickening of the basement membrane (Fig. 6D). In contrast, there was no apparent thick-

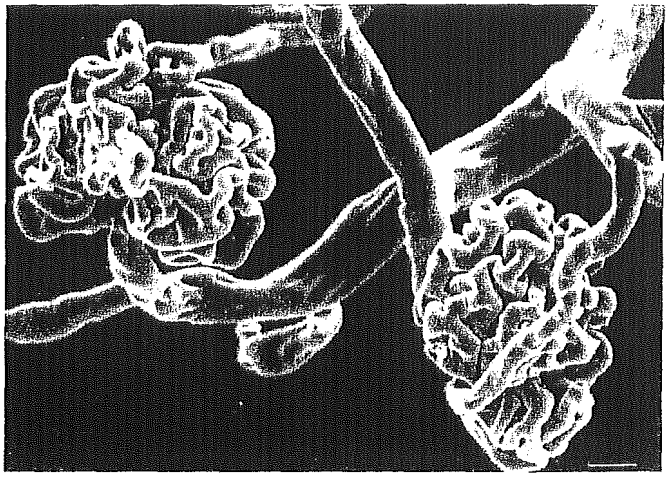

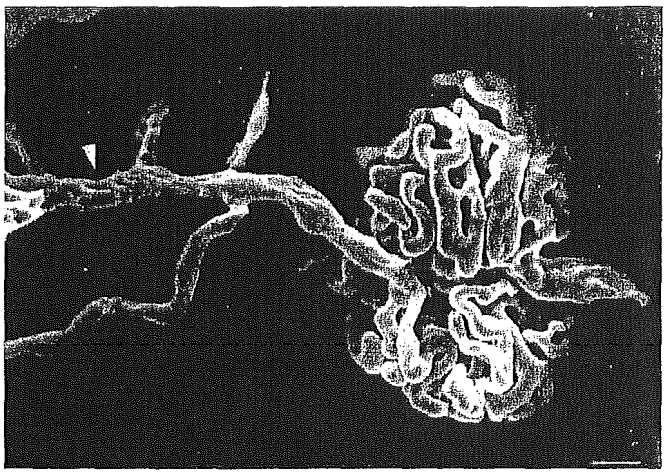

Fig. 7 Scanning electron microscopy of corrosion casts of the renal cortex of wild-type (**A**) and transgenic (**B**, **C**) mice. **B** *Arrowhead* indicates the uneven surface of the afferent arteriole in a transgenic mouse. **C** *Asterisks* indicate the cast-free space, and *arrows* indicate the club-shaped disruption of the cast in the glomerular area of a transgenic mouse. *Scale bars* 10 μm

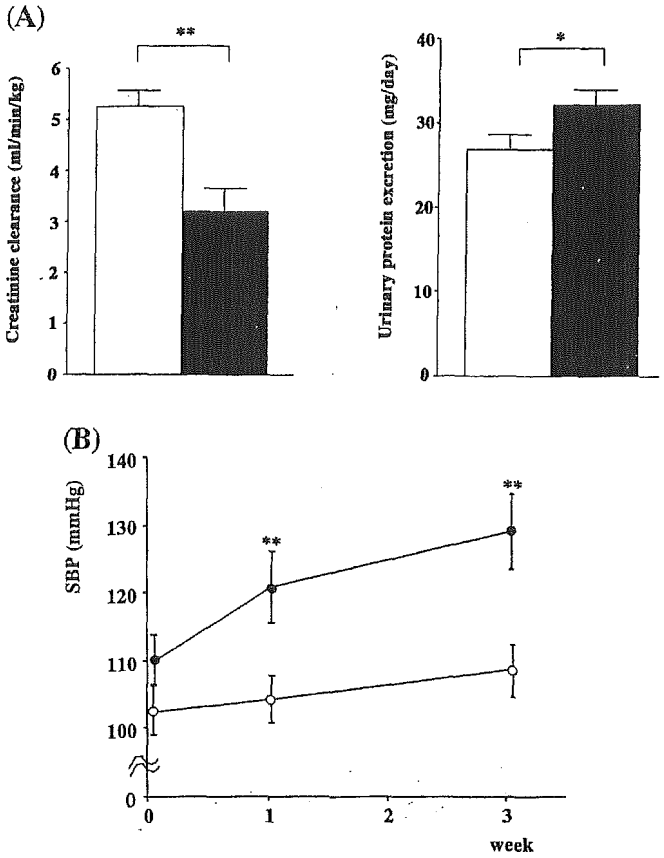

Fig. 8 **A** Creatinine clearance and urinary protein excretion of 12-month-old ET-1 transgenic (*open column*) and wild-type (*filled column*) mice (n=10 for each). **B** Time-dependent changes in BP measured in 12-month-old wild-type (*open circles*) and transgenic (*closed circles*) mice (n=10 for each) on a high-salt (8% NaCl) diet. (*SBP* Systolic blood pressure.) $^{**}P<0.01$, $^{*}P<0.05$ versus wild-type mice

ening of the basement membranes of wild-type mice (Fig. 6C).

Corrosion casts of the renal cortex

In wild-type mice, there was no narrowing or corrugation of the cast at the renal afferent and efferent arterioles; instead the surface of the cast was smooth. In areas of glomeruli, the cast was uniform in diameter and packed with complicated networks representing glomerular tufts. There were no interruptions in the cast, no clefts and no cast-free areas among the glomeruli (Fig. 7A).

In transgenic mice, by contrast, the diameter of the cast was reduced at the afferent and efferent arterioles, and its surface was uneven (Fig. 7B). Similarly, in areas of glomeruli, the cast was also irregular and reduced in diameter. Moreover, club-shaped disruptions of the cast, representing the complete occlusion of glomerular tufts, were also noted. The cast-free space was quite prominent in some glomerular areas, and might represent the hyalinization of the glomeruli (Fig. 7C).

Renal damage and salt-induced blood pressure elevation in ET-1 transgenic mice

Creatinine clearance was significantly lower in 12-month-old ET-1 transgenic mice than in wild-type mice (wild-type, 5.2±0.3 $ml \cdot min^{-1} \cdot kg^{-1}$; transgenic, 3.2±0.4 $ml \cdot min^{-1} \cdot kg^{-1}$; n=10 in each; P<0.01), and total urinary protein excretion was significantly higher in the aged transgenic mice (wild-type, 26.9±1.7 mg/day; transgenic, 32.9±1.8 mg/day; n=10 in each; P<0.05) (Fig. 8A).

When a high-salt (8% NaCl) diet was provided to 12-month-old transgenic and wild-type mice for 3 weeks, the wild-type mice showed only a slight tendency toward elevation of systolic BP. On the other hand, the systolic BP of the 12-month-old transgenic mice was significantly increased at 1 week of initiating the high-salt diet (Fig. 8B).

Discussion

By the time they were about 12 months old, ET-1 transgenic mice exhibited pronounced interstitial fibrosis, renal cysts and glomerulosclerosis, changes similar to those seen by Hocher et al. in their model [16]. Renal function, as estimated from the glomerular filtration rate, was also diminished in transgenic mice, and the increased urinary protein excretion was indicative of glomerular dysfunction. It is unlikely that the renal damage was a consequence of systemic hypertension, because the elevation of BP was significant only after high-salt loading. Electron microscopy of corrosion casts revealed the lumens of the renal afferent and efferent arterioles and the glomerular tufts to be narrowed and uneven in transgenic mice, and some of the glomeruli to be completely occluded. Vascular casting revealed similar changes in spontaneously hypertensive rats infused with ET-1 [17], making it conceivable that the renal damage was caused by local hemodynamic and arteriosclerotic changes induced by ET-1 overexpression that did not primarily affect systemic BP. With respect to glomerular filtration, ET-1 contracts afferent and efferent arterioles equally, but some evidence suggests that endogenous ET-1 predominantly affects efferent arterioles [18], which would be expected to induce intraglomerular hypertension, resulting in glomerular damage.

Nonvascular effects of ET-1 may also contribute to both the glomerulosclerosis and the interstitial fibrosis. For example, ET-1 has a potent proliferative effect on a variety of cell types, including glomerular mesangial cells [19, 20], and it promotes the synthesis of extracellular matrix [21, 22]. As mesangial and epithelial cells respectively produce mesangial and basement membrane matrices, ET-1 overproduction may directly act on these cells and cause glomerulosclerosis. Indeed, proliferation of mesangium and thickening of the basement membrane were detected by electron microscopy in the glomeruli of transgenic mice.

Aged transgenic mice typically developed three types of cystic lesions in the kidney: renal cysts, focal assemblies of small cysts and glomerular cysts. Interestingly, it was recently reported that the kidneys of Han:SPRD rats, a well-known model of human polycystic kidney disease, exhibited significantly higher levels of ET-1 than age-matched controls [23]. Thus, elevated renal ET-1 may itself contribute to cyst formation in the kidney. The renal cysts were probably a consequence of the occlusion and dilatation of the urinary tubules, but it remains unclear why the occlusion of urinary tubules was so frequent. One possibility is that the pronounced interstitial fibrosis disturbed urine passage through the urinary tubules.

On the other hand, focal assemblies of small cysts in the kidney were unique to our model. These lesions were clearly different from what are more commonly described as renal cysts, since they did not exhibit dilatation, and they were not lined with cells. Nonetheless, because degenerated cuboid cells, resembling urinary tubular cells, were scattered around them, we believe these cysts to be derived from the urinary tubules. Moreover, as the distribution of these cysts was wedge-shaped, and mainly located in regions of pronounced interstitial fibrosis, we suggest that the degeneration of the urinary tubules may have been caused by intrarenal ischemia.

Dilatation of Bowman's capsule and glomerular cysts were also detected in transgenic mice. Similar cystic lesions were observed in a chronic glomerulonephritis model induced in rat by administration of nephritogenic glycoprotein [24]. Hence, when chronically present at high levels, ET-1 may act as a nephritogenic factor.

By 12 months of age, ET-1 transgenic mice had developed salt-dependent hypertension. The observed salt-dependent hypertension would be secondary to a loss of functional units for Na^+ excretion by the kidney. It has been postulated that the progression of glomerulosclerosis exacerbates hypertension by reducing renal mass, thereby reducing the kidney's capacity to excrete Na^+.

Research into the function of ET-1 entered a new era with the clinical application of ET-1 antagonists. However, accurate estimation of the efficacy of anti-ET-1 therapy in treating human disease will require continued accumulation of both clinical and preclinical data. The present study clearly showed that mild, chronic overproduction of ET-1 is detrimental to the kidney. In the context of the pathophysiology of hypertension, ET-1 may work as a mediator, facilitating the development of renal damage, which would then exacerbate elevations in BP. If so, ET-1 antagonists may serve to attenuate hypertension-induced organ damage.

Acknowledgements This work was supported in part by a Grant-in-Aid for Scientific Research from the Ministry of Education, Science and Culture, Japan; the Program for Promotion of Fundamental Studies in Health Sciences of the Organization for Drug ADR Relief, R&D Promotion and Product Review of Japan; the Japan Cardiovascular Research Foundation; the Kanae Foundation of Research for New Medicine; TMFC; the Suzuken Memorial Foundation; the Ryoichi Naito Foundation for Medical Research; the Tokyo Biochemical Research Foundation; and the Mochida Memorial Foundation for Medical and Pharmaceutical Research.

References

1. Yanagisawa M, Kurihara H, Kimura S, Tomobe Y, Kobayashi M, Mitsui Y, Yazaki Y, Goto K, Masaki T (1988) A novel potent vasoconstrictor peptide produced by vascular endothelial cells. Nature 332:411–415
2. Masaki T (1995) Possible role of endothelin in endothelial regulation of vascular tone. Ann Rev Pharmacol Toxicol 35: 235–255
3. Levin ER (1995) Endothelins. N Engl J Med 333:356–363
4. Webb DJ, Monge JL, Rabelink TJ, Yanagisawa M (1998) Endothelin, new discoveries and rapid progress in the clinic. Trends Pharmacol Sci 19:5–8
5. Saito Y, Nakao K, Mukoyama M, Imura H (1990) Increased plasma endothelin level in patients with essential hypertension. N Engl J Med 322:205
6. McMurray JJ, Ray SG, Abdullah I, Dargie HJ, Morton JJ (1992) Plasma endothelin in chronic heart failure. Circulation 85:1374–1379
7. Koyama H, Tabata T, Nishzawa Y, Inoue T, Morii H, Yamaji T (1989) Plasma endothelin levels in patients with uraemia. Lancet 1:991–992
8. Lerman A, Edwards BS, Hallett JW, Heublein DM, Sandberg SM, Burnett JC Jr (1991) Circulating and tissue endothelin immunoreactivity in advanced atherosclerosis. N Engl J Med 325:997–1001
9. Krum H, Viskoper RJ, Lacourciere Y, Budde M, Charlon V (1998) The effect of an endothelin-receptor antagonist, bosentan, on blood pressure in patients with essential hypertension. N Engl J Med 338:784–790
10. Horio T, Kohno M, Murakawa K, Yasunari K, Yokokawa K, Ueda M, Takeda T (1991) Increased plasma immunoreactive endothelin-1 concentration in hypercholesterolemic rats. Atherosclerosis 89:239–246
11. Harats D, Kurihara H, Beloni P, Oakley H, Ziober A, Ackley D, Cain G, Kurihara Y, Lawn R, Sigal E (1995) Targeting gene expression to the vascular wall in transgenic mice using the murine preproendothelin-1 promoter. J Clin Invest 95:1335–1344
12. Maemura K, Kurihara H, Kurihara Y, Oda H, Ishikawa T, Copeland NG, Gilbert DJ, Jenkins NA, Yazaki Y(1996) Sequence analysis, chromosomal location and developmental expression of the mouse preproendothelin-1 gene. Genomics 31:177–184
13. Matsumoto H, Suzuki N, Onda H, Fujino M (1989) Abundance of endothelin-3 in rat intestine, pituitary gland and brain. Biochem Biophys Res Commun 164:74–80
14. Suzuki N, Matsumoto H, Kitada C, Masaki T, Fujino M (1989) A sensitive sandwich-enzyme immunoassay for human endothelin. J Immunol Methods 118:245–250
15. Sugimoto K, Fujimura A, Takasaki I, Tokita Y, Iwamoto T, Takizawa T, Gotoh E, Shionoiri H, Ishii M (1998) Effects of renin-angiotensin system blockade and dietary salt intake on left ventricular hypertrophy in Dahl salt-sensitive rats. Hypertens Res 21:163–168
16. Hocher B, Thone-Reineke C, Rohmeiss P, Schmager F, Slowinski T, Burst V, Siegmund F, Quertermous T, Bauer C, Neumayer HH, Schleuning WD, Theuring F (1997) Endothelin-1 transgenic mice develop glomerulosclerosis, interstitial fibrosis, and renal cyts but not hypertension. J Clin Invest 99:1380–1389
17. Hirata Y, Matsuoka H, Kimura K, Fukui K, Hayakawa H, Suzuki E, Sugimoto T, Sugimoto T, Yanagisawa M, Masaki T (1989) Renal vasoconstriction by the endothelial cell-derived peptide endothelin in spontaneously hypertensive rats. Circ Res 65:1370–1379
18. Haynes WG, Webb DJ (1998) Endothelin as a regulator of cardiovascular function in health and disease. J Hypertens 16: 1081–1098
19. Simonson MS, Wann S, Mene P, Dubyak GR, Kester M, Nakazato Y, Sedor JR, Dunn MJ (1989) Endothelin stimulates phospholipase C, Na+/H+ exchange, c-fos expression, and mitogenesis in rat mesangial cells. J Clin Invest 83:708–712
20. Badr KF, Murray JJ, Breyer MD, Takahashi K, Inagami T, Harris RC (1989) Mesangial cell, glomerular and renal vascular responses to endothelin in the rat kidney. Elucidation of signal transduction pathways. J Clin Invest 83:336–342
21. Gomez-Garre D, Ruiz-Ortega M, Ortego M, Largo R, Lopez-Armada MJ, Plaza JJ, Gonzalez E, Egido J (1996) Effects and interactions of endothelin-1 and angiotensin II on matrix protein expression and synthesis and mesangial cell growth. Hypertension 27:885–892
22. Zhuo J, Dean R, Maric C, Aldred PG, Harris P, Alcorn D, Mendelsohn FA (1998) Localization and interactions of vasoactive peptide receptors in renomedullary interstitial cells of the kidney. Kidney Int 67:S22–S28
23. Hocher B, Zart R, Braun N, Schwarz A, van der Woude F, Rohmeiss P, Koppenhagen K (1998) The Endothelin system in polycystic kidneys of Han:SPRD rats. J Cardiovasc Pharmacol 31[Suppl. 1]:S342–S344
24. Natori Y, Shibata S (1986) Comparison of nephritogenic glycopeptide, nephritogenoside, isolated from rat glomerular basement membranes with other basement membrane components. Connect Tissue Res 15:245–255

British Journal of Pharmacology (2002) 137, 621–628
www.nature.com/bjp

Role of the platelet-activating factor (PAF) receptor during pulmonary infection with gram negative bacteria

[1]A.C. Soares, [1]V.S. Pinho, [1]D.G. Souza, [2,3]T. Shimizu, [2,3]S. Ishii, [4]J.R. Nicoli & *,[1]M.M. Teixeira

[1]Immunopharmacology Laboratory, Departamento de Bioquímica e Imunolgia, ICB, Universidade Federal de Minas Gerais, Belo Horizonte, Brazil; [2]Department of Biochemistry and Molecular Biology, Faculty of Medicine, The University of Tokyo, Japan; [3]CREST of Japan Science and Technology Corporation, Tokyo, Japan and [4]Departamento de Microbiologia, ICB, Universidade Federal de Minas Gerais, Belo Horizonte, Brazil

1 The lipid mediator PAF plays an important role in the phagocytosis of particles, including bacteria, and consequent production of pro-inflammatory cytokines, such as TNF-α and IL-8.

2 Using a PAF receptor antagonist (UK-74,505) and PAF receptor knock-out mice, we have investigated the relevance of PAF for the inflammatory changes and lethality after pulmonary infection with the gram-negative bacteria *Klebsiella pneumoniae* in mice.

3 At an inoculum of 3×10^6 bacteria, there was marked pulmonary (bronchoalveolar lavage and lung) neutrophilia that started early (2.5 h after infection) and peaked at 48 h. All animals were dead by day 4 of infection. The chemokine KC and the pro-inflammatory cytokine TNF-α increased rapidly and persisted for 48 h in the lungs.

4 Pretreatment with UK-74,505 (30 mg kg^{-1} per day, p.o.) had no significant effects on the number of infiltrating neutrophils in BAL fluid or lung tissue, as assessed by histology and measuring myeloperoxidase, or on the concentrations of KC. In contrast, concentrations of TNF-α and the number of bacteria inside neutrophils were significantly diminished.

5 In order to support a role for the PAF during *K. pneumoniae* infection, experiments were also carried out in PAFR-deficient mice. In the latter animals, lethality occurred earlier than in wild-type controls. This was associated with greater number of bacteria in lung tissue and diminished percentage of neutrophils containing bacteria in their cytoplasm.

6 Our results suggest that PAF, acting on its receptor, plays a protective role during infection with *K. pneumoniae* in mice.

British Journal of Pharmacology (2002) **137**, 621–628. doi:10.1038/sj.bjc.0704918

Keywords: Chemokines; lung inflammation; neutrophils; TNF-α; recruitment

Abbreviations: BAL, bronchoalveolar lavage; CFU, colony forming units; KC, keratinocyte-derived chemokine; LPS, lipopolysaccharide; MCP-1, monocyte chemoattractant protein-1; MPO, myeloperoxidase; PAF, platelet activating factor; PAFR, PAF receptor; $PAFR^{-/-}$, PAF receptor-deficient mice; PBS, phosphate buffered saline; PMN, polymorphonuclear leukocyte; TNF-α, tumour necrosis factor-α

Introduction

Platelet-activating factor (PAF, 1-O-alkyl-2-acetyl-sn-glycero-3-phosphocholine) is a potent autacoid lipid mediator with various biological activities, including platelet and leukocyte activation. PAF acts by binding to a G protein-coupled seven transmembrane receptor, the PAF receptor (PAFR), and appears to regulate constitutively various physiological processes (Ishii & Shimizu, 2000). In addition to its role as a physiological mediator, PAF has been shown to play an important role in the pathophysiology of various inflammatory conditions (Ishii & Shimizu, 2000). Studies with PAFR antagonists or PAFR-deficient animals have shown an essential role of PAFR during systemic allergic anaphylaxis-associated shock in mice (Ishii & Shimizu, 2000; Montrucchio *et al.*, 2000). Studies with PAFR antagonists or strategies that decrease PAF activity have also demonstrated an important role of PAF for lipopolysaccharide (LPS)-induced shock and lethality (e.g. Fukuda *et al.*, 2000) and for the lung injury which follows a range of inflammatory stimuli (Miotla *et al.*, 1998; Tavares-de-Lima *et al.*, 1998; De Matos *et al.*, 1999).

More recently, we have suggested an important role of PAFR for the protective immune response of the murine host against infection with an intracellular protozoan parasite, *T. cruzi* (Aliberti *et al.*, 1999). In the latter system, PAF induced NO release by *T. cruzi*-infected macrophages *in vitro* and pretreatment of mice with PAFR antagonists increased blood parasitaemia and enhanced infection-associated lethality (Aliberti *et al.*, 1999). These results are in line with the ability of leukocytes to produce PAF upon encounter with microorganisms or soluble particles and to engulf them in a PAF-dependent manner (Makristathis *et al.*, 1993; Au *et al.*, 2001). Moreover, exposure of leukocytes to endotoxin or bacteria may trigger PAF release (reviewed by Montrucchio *et al.*, 2000; Makristathis *et al.*, 1993). Thus, it is clear that PAF may have a dual role during bacterial

*Author for correspondence at: Immunofarmacologia, Departamento de Bioquímica e Imunologia, Instituto de Ciencias Biologicas, Universidade Federal de Minas Gerais, Av. Antonio Carlos. 6627 - Pampulha, 31270-901 Belo Horizonte MG Brasil;
E-mail: mmtex@icb.ufmg.br

infections. On one hand, PAF appears to play an important role in the ability of a host to deal with infections by facilitating phagocytosis and killing of engulfed microorganisms. On the other hand, PAFR activation may underlie the tissue injury and shock associated with the infection and endotoxin released.

In this study, we have investigated the relevance of PAF receptors in a model of pulmonary infection in mice caused by gram-negative bacteria. Thus, we have assessed the effects of the treatment with a PAFR antagonist, UK-74,505, on the lethality bacterial counts and inflammatory indices following pulmonary infection of mice with *Klebsiella pneumoniae*. UK-74,505 is a potent, specific, orally available and long-acting PAFR antagonist (Alabaster *et al.*, 1991; Parry *et al.*, 1994; Jezequel *et al.*, 1996). For comparison, we also assessed the lethality and infection indices of $PAFR^{-/-}$ mice after infection with *K. pneumoniae*.

Methods

Animals

Balb/C (8 to 12 week-old) female mice obtained from the Bioscience unit of our Institution were housed in standard conditions and had free access to commercial chow and water. PAF receptor-deficient ($PAFR^{-/-}$) mice were generated as previously described and backcrossed or at least 10 generations into a Balb/C background (Ishii *et al.*, 1998). All procedures described here had prior approval from the animal ethics committee of Instituto de Ciências Biológicas (Belo Horizonte, Brazil).

Bacteria

The bacterium used was *Klebsiella pneumoniae* – ATCC 27 736 that has been kept in the Department of Microbiology, Universidade Federal de Minas Gerais. Before the experiments described herein, bacteria were made pathogenic by 10 passages in Balb/C mice (i.p. injection and collection in the spleen 24 h later) and kept frozen in a −70°C freezer at a concentration of 1×10^9 CFU ml^{-1} in tryptic soy broth containing 10% glycerol (v v^{-1}) until use. Bacteria were frozen when in the log phase of growth.

Treatment with UK-74,505

The PAF receptor antagonist UK-74,505 (modipafant, a gift of Dr J. Parry, Pfizer, Sandwich, U.K.) was dissolved initially in 0.1 M HCl and further diluted 10 fold in saline. Control animals received an oral administration of vehicle (0.01 M HCl), whereas the test group received an oral administration of UK-74,505 at dose of 30 mg kg^{-1}. The oral dose chosen was recommended by the supplier and has been previously shown to give good bioavailability for 24 h (Alabaster *et al.*, 1991; Parry *et al.*, 1994; Jezequel *et al.*, 1996). For lethality experiments, the drug was administered 24 and 2 h prior to inoculation of bacteria and daily thereafter. For the experiments measuring infection and inflammatory indices, the drug was administered 24 and 2 h prior to inoculation of bacteria and animals sacrificed 24 h after inoculation.

K. pneumoniae *inoculation*

K. pneumoniae was grown in tryptic soy broth (Difco, Detroit, MI, U.S.A.) for 18 h at 37°C prior to inoculation. The concentration of bacteria in broth was routinely determined by serial 1 : 10 dilutions. One hundred microlitres of each dilution were plated on McConkey agar plates and incubated for 24 h at 37°C and then colonies were counted. Each animal was anaesthetized i.p. with 0.2 ml of a solution containing xylazin (0.002 mg ml^{-1}), ketamin (50 mg ml^{-1}) and saline in a proportion of 1 : 0.5 : 3, respectively. The trachea was exposed and 30 μl of a suspension containing 3×10^6 *K. pneumoniae* or saline was administered with a sterile 26-gauge needle. The skin incision was closed with surgical staples.

Bronchoalveolar lavage

Bronchoalveolar lavage (BAL) was performed to obtain leukocytes in the alveolar spaces. The trachea was exposed and a 1.7-mm-outside-diameter polyethylene catheter inserted. BAL was performed by instilling three 1-ml aliquots of PBS and approximately 2 ml of fluid was retrieved per mouse. The number of total leukocytes was determined by counting leukocytes in a modified Neubauer chamber after staining with Turk's solution. Differential counts were obtained from cytospin preparations by evaluating the percentage of each leukocyte on a slide stained with May-Grunwald-Giemsa. In some experiments, the percentage of BAL neutrophils that had phagocytosed at least one bacterium was evaluated in at least 200 cells.

Determination of myeloperoxidase activity

The extent of neutrophil accumulation in the lung tissue was measured by assaying myeloperoxidase activity as previously described (De Matos *et al.*, 1999). Using the conditions described below, this methodology is very selective for the determination of neutrophils over macrophages (data not shown). Briefly, a portion of left lungs of animals was removed and snap frozen in liquid nitrogen. Upon thawing, the tissue (0.1 g of tissue per 1.9 ml of buffer) was homogenized in pH 4.7 buffer (0.1 M NaCl, 0.02 M $NaPO_4$, 0.015 M NaEDTA), centrifuged at $3000 \times g$ for 10 min and the pellet subjected to hypotonic lyses (1.5 ml of 0.2% NaCl solution followed 30 s later by addition of an equal volume of a solution containing NaCl 1.6% and glucose 5%). After a further centrifugation, the pellet was resuspended in 0.05 M $NaPO_4$ buffer (pH 5.4) containing 0.5% hexadecyltrimethylammonium bromide (HTAB) and re-homogenized. One millilitre aliquots of the suspension were transferred into 1.5 ml-Eppendorf tubes followed by three freeze-thaw cycles using liquid nitrogen. The aliquots were then centrifuged for 15 min at $3000 \times g$, the pellet was resuspended to 1 ml and samples of lung were diluted (1 : 20) prior to assay. Myeloperoxidase (MPO) activity in the resuspended pellet was assayed by measuring the change in optical density (O.D.) at 450 nm using tetramethylbenzidine (1.6 mM) and H_2O_2 (0.5 mM). Results were expressed as 'myeloperoxidase index' and were calculated by comparing the O.D. of tissue supernatant with the O.D. of mouse peritoneal neutrophils processed in the same way. To this

end, neutrophils were induced in the peritoneum of mouse by injecting 3 ml of casein 5%. A standard curve of neutrophil (>95% purity) numbers versus O.D. was obtained by processing purified neutrophils as above and assaying for MPO activity.

Determination of plasma and lung K. pneumoniae *colony forming units*

At time of sacrifice, plasma was collected from the branchial plexus, the right ventricle was perfused with 3 ml of sterile saline and lungs were harvested. Tissues were then homogenized with a homogenizer in a vented hood. The homogenates and plasma were placed on ice, and serial 1:10 dilutions were made. One hundred microlitres of each dilution were plated on McConkey agar plates (Difco) and incubated for 24 h at 37°C and then the number of colony forming units (CFU) was counted. The detection limit of the assay was 100 bacteria ml^{-1} or 100 bacteria per 100 mg of tissue.

Harvesting of lungs and blood for cytokine analysis

At the designated time point, mice were anaesthetized with xylazin/ketamin/saline as above, blood collected from the brachial plexus and the animals sacrificed. Prior to lung removal, the pulmonary vasculature was perfused with 3 ml of PBS *via* the right ventricle. The right lung was then harvested for assessment of the various cytokine protein levels.

Measurement of cytokine concentrations in serum, BAL and lungs

The cytokine concentrations (TNF-α, KC, MCP-1/JE) were measured in serum, BAL and lung of animals using ELISA techniques with commercially available antibodies and according to the instructions supplied by the manufacturer (R&D Systems). Serum was obtained from coagulated blood (15 min at 37°C, then 30 min at 4°C) and stored at −20°C until further analysis. Serum and BAL samples were analysed at a 1:3 and 1:5 dilution in assay dilution buffer, respectively. One hundred milligrams of lung of controls and treated animals were homogenized in 1 ml of PBS (0.4 m NaCl and 10 mM $NaPO_4$) containing anti-proteases (0.1 mM PMSF, 0.1 mM benzethonium chloride, 10 mM EDTA and 20 KI aprotinin A) and 0.05% Tween 20. The samples were then centrifuged for 10 min at $3000 \times g$ and the supernatant immediately used for ELISA assays at a 1:5 dilution in assay dilution buffer. The detection limit of the ELISA assays was 16 pg ml^{-1}.

Determination of the levels of circulating leukocytes

The total number of circulating leukocytes and neutrophils were evaluated in blood samples obtained at the end of the experiments described in Figure 1. The number of total circulating leukocytes was determined by counting leukocytes in a modified Neubauer chamber after staining with Turk's solution and differential counts by evaluating the percentage of each leukocyte on blood films stained with May-Grunwald-Giemsa.

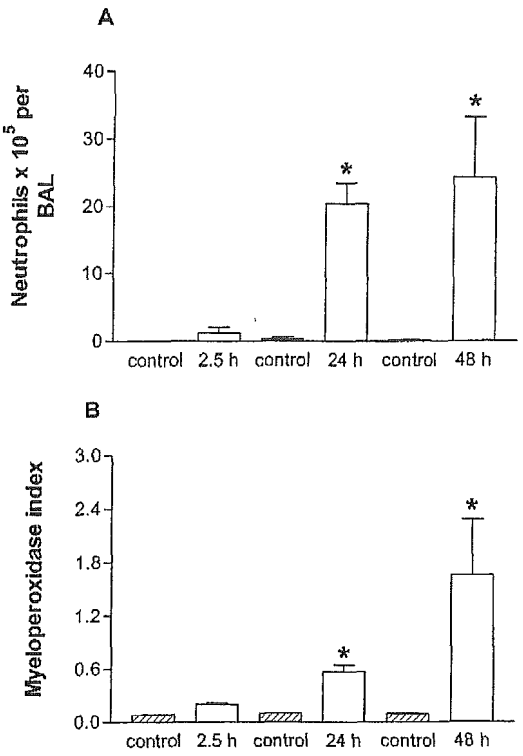

Figure 1 Kinetics of the influx of neutrophils in the lungs of mice infected with *K. pneumoniae*. Animals were inoculated with 3×10^6 bacteria or vehicle (30 μl) and neutrophil influx in (A) in the bronchoalveolar lavage (BAL) fluid or (B) lungs assessed after 2.5, 24 and 48 h. Myeloperoxidase (MPO) activity in lungs was used as an index of neutrophil influx in that tissue. Results are shown as the number of neutrophils or leukocyte index and represent the mean±s.e.mean of six animals in each group. $*P<0.01$ when compared with uninfected animals.

Histology

Lungs were inflated with 2 ml phosphate-buffered 10% formalin, embedded in paraffin and 4 μm-thick sections obtained. The sections were then stained with haematoxylin and eosin and examined under a light microscope.

Statistical analysis

Results are shown as means±s.e.mean. Data sets were compared by using analysis of variance (ANOVA) followed by Student-Newman-Keuls *post hoc* analysis. Results were considered significant when $P<0.05$.

Results

Kinetics of the pulmonary inflammation and infection after intratracheal (i.t.) inoculation of K. pneumoniae

Initial experiments were carried out to characterize the kinetics of the pulmonary response after instillation of *K. pneumoniae*. Mice were injected with 30 μl of a saline suspension containing 3×10^6 bacteria, an inoculum shown to be optimal for inducing lung inflammation and survival of animals for at least 48 h (data not shown). Twenty-four